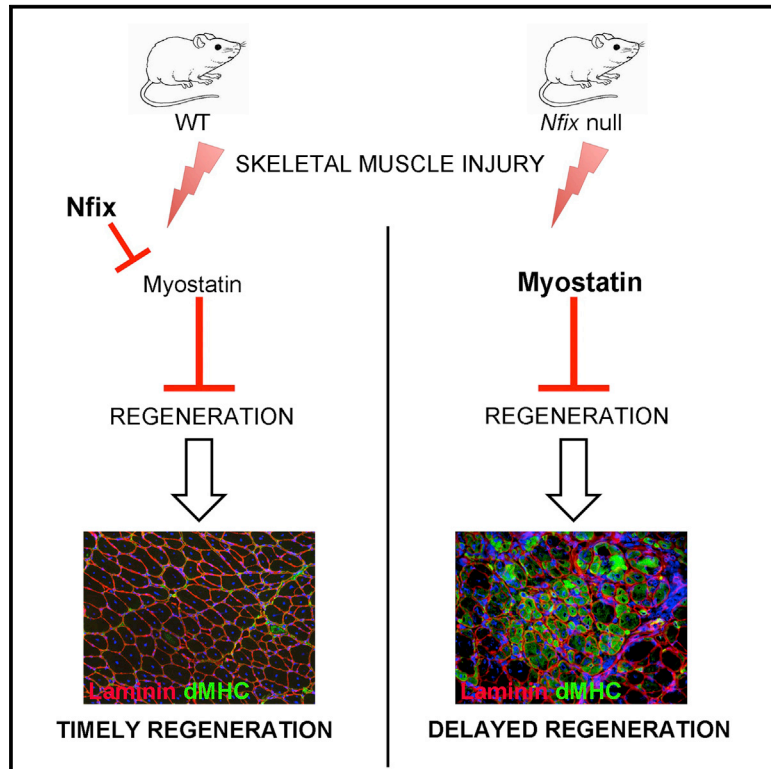


## Nfix Regulates Temporal Progression of Muscle Regeneration through Modulation of Myostatin Expression

### Graphical Abstract



### Authors

Giuliana Rossi, Stefania Antonini, Chiara Bonfanti, ..., Shahrugim Tajbakhsh, Giulio Cossu, Graziella Messina

### Correspondence

graziella.messina@unimi.it

### In Brief

Rossi et al. highlight a function for Nfix during postnatal skeletal muscle regeneration and a link with Myostatin. During regeneration, Nfix regulates Myostatin expression, thus controlling the temporal progression of the regeneration process. When Nfix is deficient, regeneration is markedly delayed.

### Highlights

- Muscle differentiation is delayed in *Nfix*-null satellite cells in vitro
- Mice lacking Nfix in satellite cells show delayed regeneration upon injury
- Nfix directly regulates Myostatin expression during regeneration
- In vivo silencing of Myostatin rescues the regeneration deficit in *Nfix*-null mice



# Nfix Regulates Temporal Progression of Muscle Regeneration through Modulation of Myostatin Expression

Giuliana Rossi,<sup>1</sup> Stefania Antonini,<sup>1</sup> Chiara Bonfanti,<sup>1</sup> Stefania Monteverde,<sup>1</sup> Chiara Vezzali,<sup>1</sup> Shahragim Tajbakhsh,<sup>2</sup> Giulio Cossu,<sup>1,3</sup> and Graziella Messina<sup>1,\*</sup>

<sup>1</sup>Department of Biosciences, University of Milan, Via Celoria 26, 20133 Milan, Italy

<sup>2</sup>Stem Cells and Development, Department of Developmental & Stem Cell Biology, CNRS UMR 3738, Institut Pasteur, 25 Rue du Dr. Roux, 75015 Paris, France

<sup>3</sup>Institute of Inflammation and Repair, University of Manchester, Oxford Road, M13 9PL Manchester, UK

\*Correspondence: [graziella.messina@unimi.it](mailto:graziella.messina@unimi.it)

<http://dx.doi.org/10.1016/j.celrep.2016.02.014>

This is an open access article under the CC BY-NC-ND license (<http://creativecommons.org/licenses/by-nc-nd/4.0/>).

## SUMMARY

Nfix belongs to a family of four highly conserved proteins that act as transcriptional activators and/or repressors of cellular and viral genes. We previously showed a pivotal role for Nfix in regulating the transcriptional switch from embryonic to fetal myogenesis. Here, we show that Nfix directly represses the Myostatin promoter, thus controlling the proper timing of satellite cell differentiation and muscle regeneration. *Nfix*-null mice display delayed regeneration after injury, and this deficit is reversed upon in vivo Myostatin silencing. Conditional deletion of *Nfix* in satellite cells results in a similar delay in regeneration, confirming the functional requirement for Nfix in satellite cells. Moreover, mice lacking Nfix show reduced myofiber cross sectional area and a predominant slow twitching phenotype. These data define a role for Nfix in postnatal skeletal muscle and unveil a mechanism for Myostatin regulation, thus providing insights into the modulation of its complex signaling pathway.

## INTRODUCTION

Skeletal muscles play a critical role in voluntary movement, and proper regeneration of this tissue after injury can be severely compromised in a variety of contexts including neuromuscular disorders. In vertebrates, muscle progenitors originating from presomitic and cranial mesoderm give rise to “embryonic” or primary myogenesis, necessary to establish the basic muscle pattern, and “fetal” secondary myogenesis, characterized by growth and maturation of the muscle masses and by onset of innervation (Biressi et al., 2007a). These two waves of myogenesis are mediated by distinct embryonic and fetal myoblasts, respectively, each characterized by differentially expressed genes and properties of the myoblasts as well as the differentiated cells that they produce (Biressi et al., 2007b; Hutcheson

et al., 2009). A key regulator of the embryonic and fetal classes is Nuclear Factor I X (*Nfix*), which is abundant in the fetus and almost absent in the embryo (Biressi et al., 2007b; Messina et al., 2010). Nfix drives the transcriptional changes from embryonic to fetal myogenesis by specifically repressing embryonic and activating fetal specific genes (Messina et al., 2010), and its role is partially conserved during evolution (Pistocchi et al., 2013).

Nfix is part of a family of highly conserved DNA-binding proteins that function as transcriptional activators and/or repressors: *Nfia*, *Nfib*, *Nfic*, and *Nfix*. NFI-binding sites are present in the promoter, enhancer and silencer regions of many cellular and viral genes (Kruse and Sippel, 1994), and NFI binding motifs were detected in promoters of genes expressed in different organs, such as brain (Bedford et al., 1998), lung (Bachurski et al., 1997), liver (Jackson et al., 1993), intestine (Xu et al., 2005), muscle (Spitz et al., 1997), connective tissue and skeletal elements (Szabó et al., 1995). *Nfix*-null mice are characterized by a reduced body size and inability to fully extend their limbs as well as CNS and skeletal deficits (Campbell et al., 2008; Driller et al., 2007). NFI binding sites are present in the promoters of the differentiation gene *Myogenin* and muscle-specific phosphofructo-kinase (Darville et al., 1992; Edmondson et al., 1992), and they can form a complex with Myogenin, thus increasing their affinity for muscle-specific genes (Funk and Wright, 1992; Johanson et al., 1999).

Another critical regulator of prenatal and postnatal myogenesis is Myostatin, a secreted factor of the TGF $\beta$  superfamily that was shown to be a negative regulator of muscle size, where loss-of-function mutations result in a dramatic increase in muscle mass in different species including human (McPherron et al., 1997; McPherron and Lee, 1997; Schuelke et al., 2004). Although interference of this pathway was reported to lead to functional improvement of dystrophic muscles in mice (Bogdanovich et al., 2002), the precise mode of action of this powerful signaling pathway as a potential therapeutic agent for myopathies remains unclear. Notably, the contextual role of Myostatin was highlighted, where in the embryo it regulates the balance between proliferation and differentiation of muscle progenitors (Manceau et al., 2008), whereas in the adult, opposing roles in

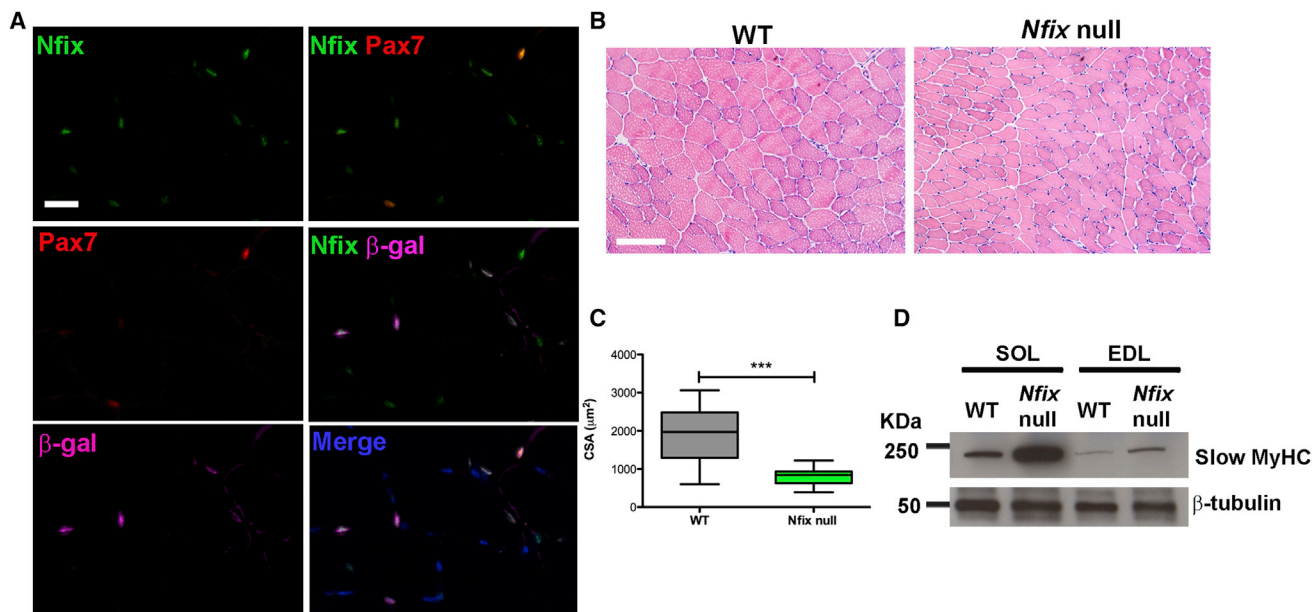


**Figure 1. Nfix Is Expressed by SCs and Its Absence Leads to a Reduced Myofiber Cross Sectional Area and to an Increased Slow MyHC Expression**

(A) Immunofluorescence analysis of Nfix expression (green) in Pax7<sup>+</sup> SCs (red) on a *Tibialis anterior* muscle section of a *Mic3f-lacZ* mouse, where myonuclei are in purple (β-gal). Hoechst was used to stain nuclei (n = 4 mice). The scale bar represents 25 μm.

(B) H&E staining on *Tibialis anterior* muscles from WT and *Nfix*-null mice (n = 5 mice). The scale bar represents 100 μm.

(C) Graphical representation of the myofiber cross sectional area (CSA) in WT and *Nfix*-null muscles. The plotted values represent the distribution of n = 65 measurements on five random microscope fields (\*\*p < 0.001 and two-tailed unpaired t test). The data are presented as mean ± whiskers from min to max.

(D) Western blot analysis of slow MyHC expression in WT and *Nfix*-null *Soleus* (SOL) and EDL muscles. The β-tubulin was used to normalize.

See also Figure S1.

regulating myogenic differentiation have been reported (Langley et al., 2002; Thomas et al., 2000; McCroskery et al., 2003; Taylor et al., 2001).

Postnatal myogenesis is assured by satellite cells (SCs) that are located between the basal lamina and the myofiber plasma membrane (Mauro, 1961). Although they account for less than 5% of total muscle nuclei in adult muscles, they play an indispensable role in the regeneration of adult skeletal muscle (Lepper et al., 2011; McCarthy et al., 2011; Murphy et al., 2011; Relaix and Zammit, 2012; Sambasivan et al., 2011).

Here, we report that absence of Nfix provokes an imbalance in skeletal muscle homeostasis and regeneration. Moreover, we identify Nfix as a regulator of Myostatin, where in vivo silencing of Myostatin in regenerating *Nfix*-null muscles rescues the regeneration defect. These findings have broad implications for the understanding of pathways regulating postnatal myogenesis and regeneration as well as providing insights into the role of Myostatin as a critical regulator of skeletal muscle differentiation.

## RESULTS

### Altered Skeletal Muscle Phenotype in *Nfix*-Null Mice

We demonstrated previously that Nfix plays a critical role in the switch from embryonic to fetal myogenesis (Messina et al., 2010). Interestingly, *Nfix*-null mice are characterized by reduced body size and inability to fully extend their limbs, suggesting a

possible muscular phenotype (Driller et al., 2007). To explore the role of Nfix in adult myogenesis, we examined its expression and observed that both myonuclei and Pax7<sup>+</sup> SCs express Nfix (Figure 1A). Histological analysis of *Nfix*-null muscles showed a marked reduction in the cross sectional area of myofibers, although general muscle architecture remained normal compared to wild-type littermates (Figures 1B and 1C). In addition, *Nfix*-null SC-derived myoblasts were able to differentiate in vitro (Figure S1A), with no significant difference in proliferation and apoptosis rates with respect to the wild-type (Figures S1B and S1C). We reported previously that the embryonic marker slow MyHC is negatively regulated by Nfix, through repression of its activator Nfatc4 (Messina et al., 2010). Interestingly, adult muscles lacking Nfix were characterized by an increased expression of slow MyHC, which is evident in both typically slow-twitching muscles (such as the *Soleus*) and fast-twitching muscles (such as the EDL, *Extensor Digitorum Longus*) (Figure 1D). Notably, *Nfix*-null differentiated SC-derived myotubes in vitro also expressed higher levels of slow MyHC compared to wild-type (Figure S1D).

### SC Differentiation and Muscle Regeneration Are Delayed in the Absence of Nfix

To assess the role of Nfix during regeneration, we first examined single muscle fibers isolated from wild-type and *Nfix*-null mice. Freshly isolated wild-type and *Nfix*-null single fibers had

comparable numbers of associated Pax7<sup>+</sup> SCs (Figure S2A) and after 24 hr in culture the number of MyoD expressing cells was similar (Figure S2B). Analysis of SC proliferation and percentage of MyoD expression during the first 12 hr in culture revealed no difference between the two groups (Figures S2C and S2D). Although no significant alterations in numbers of Pax7<sup>+</sup> and MyoD<sup>+</sup> SCs were noted on *Nfix*-null myofibers, immunostaining for MyoD and Myogenin on wild-type and *Nfix*-null myofibers showed a marked reduction in the number of double MyoD<sup>+</sup>/Myogenin<sup>+</sup> cells in absence of *Nfix* (Figures 2A and 2B). Notably, this loss of differentiated cells in *Nfix*-null myofibers was more pronounced after 72 hr in culture, suggesting a possible involvement of *Nfix* during SC differentiation. Interestingly, the reduction in Myogenin<sup>+</sup> cells was less evident at later stages (Figure 2B), thus suggesting a delay in muscle differentiation rather than a general block of the differentiation process.

We reasoned that a delay in myogenic differentiation in absence of *Nfix* could result in an altered regeneration in vivo. We therefore injected the *Tibialis anterior* muscle of wild-type and *Nfix*-null mice with the snake venom cardiotoxin (CTX) to induce muscle regeneration. Following tissue damage, we observed a striking delay in muscle regeneration after injury of *Nfix*-null mice, as observed by persistent expression of developmental MyHC (Collins et al., 2005; Sartore et al., 1982; Schiaffino et al., 1986) (dMHC) expression (Figures 3A and 3D). In addition, the *Nfix*-null exhibited smaller regenerating myofibers compared to wild-type (Figure S2E). Accordingly, Myogenin expression was delayed and protracted in *Nfix*-null muscles (Figure 3B), in keeping with our in vitro observations (Figures 2A and 2B). Nevertheless, in spite of this altered timing, muscle regeneration appeared complete at later time points in the *Nfix*-null (28 days after injury, see Figure 3A). Interestingly, in *Nfix*-null mice, we observed a marked upregulation of Myostatin, a potent inhibitor of myogenesis, suggesting that this signaling pathway might be involved in the delayed muscle regeneration phenotype (Figure 3B). This was most evident from day 5 after CTX injection at a time when differentiation has already initiated, and it was accompanied by the upregulation of the Myostatin downstream effector phosphorylated Smad3 (pSmad3), particularly after 7 days (Figure 3C), suggesting a functional role for Myostatin signaling. These results clearly indicate a role for *Nfix* in regulating the proper timing of Myostatin expression and, in turn, of muscle regeneration upon injury. Analysis of Myostatin expression in uninjured muscles revealed no difference between wild-type and *Nfix*-null animals (data not shown), suggesting that the upregulation of Myostatin expression specifically occurs as a consequence of muscle injury.

### Specific Deletion of *Nfix* in SCs Recapitulates the Regeneration Defects

Since *Nfix* expression is not restricted to SCs, we investigated muscle regeneration after CTX injury in tamoxifen treated *Tg:Pax7-Cre<sup>ERT2</sup>:Nfix<sup>fl/fl</sup>* mice (see Figure S3A) to examine the specific role of *Nfix* in Pax7<sup>+</sup> SCs. Tamoxifen treated *Tg:Pax7-Cre<sup>ERT2</sup>:Nfix<sup>fl/fl</sup>* mice were compared with both tamoxifen untreated mice and mice expressing only the *Tg:Pax7-Cre<sup>ERT2</sup>* allele and treated with tamoxifen, as controls. To verify the efficacy of tamoxifen treatment, sections of regenerating mouse

muscles from each group were stained for *Nfix*. In both *Tg:Pax7-Cre<sup>ERT2</sup>:Nfix<sup>+/+</sup>* and tamoxifen untreated *Tg:Pax7-Cre<sup>ERT2</sup>:Nfix<sup>fl/fl</sup>* mice, all the centrally nucleated myofibers were *Nfix<sup>+</sup>*, as expected (Figure S3C). In tamoxifen treated *Tg:Pax7-Cre<sup>ERT2</sup>:Nfix<sup>fl/fl</sup>* mice, *Nfix* expression was completely abolished in regenerating myonuclei, while it was still present in non-muscle nuclei, thereby confirming the specificity of *Tg:Pax7-Cre<sup>ERT2</sup>* deletion (Figure S3C). Efficiency of *Nfix* deletion was also measured by counting the percentage of Pax7<sup>+</sup> cells that had excised *Nfix* and was calculated to be 96.2% ± 0.4 (Figure S3D). Notably, tamoxifen treated *Tg:Pax7-Cre<sup>ERT2</sup>:Nfix<sup>fl/fl</sup>* mice showed a delayed regeneration when compared to both tamoxifen untreated floxed mice and tamoxifen treated *Nfix<sup>+/+</sup>* mice (Figure 4A). This defective regeneration was evident in tamoxifen treated *Tg:Pax7-Cre<sup>ERT2</sup>:Nfix<sup>fl/fl</sup>* mice at 7 and 14 days post-CTX injection where dMHC expression persisted, and H&E sections revealed the continued presence of necrotic and inflammatory areas (Figures 4A and S3E). Further, the analysis of Myogenin clearly showed protracted expression in the tamoxifen treated *Tg:Pax7-Cre<sup>ERT2</sup>:Nfix<sup>fl/fl</sup>* mice, confirming the delay in the regenerative process (Figure 4B). Finally, the distribution of the cross sectional area of regenerating myofibers in the three groups supports the delayed regeneration phenotype of tamoxifen treated *Tg:Pax7-Cre<sup>ERT2</sup>:Nfix<sup>fl/fl</sup>* mice, mostly evident after 14 days (Figure S3B). These data support the specific function of *Nfix* in SCs for proper timing of Myogenin expression as well as the regeneration process.

### *Nfix* Regulates Myostatin Expression in Differentiating Myoblasts

In keeping with the observation that *Nfix*-null mice exhibit delayed muscle regeneration, Myostatin expression was upregulated in the absence of *Nfix* (Figure 3B). Since Myostatin is a TGF-β family member with anti-myogenic properties (Elliott et al., 2012), its upregulation can explain the delayed regeneration observed in mice lacking *Nfix*. To address this point, we investigated the possibility that *Nfix* might directly regulate Myostatin expression in differentiating myoblasts. First, we analyzed Myostatin expression in differentiating SC-derived myoblasts. As shown in Figure 5A, *Nfix* acts as a suppressor of Myostatin in differentiating myoblasts, even in absence of the contribution of the myofiber.

For biochemical analysis, we validated this result using the C2C12 myogenic cell line. C2C12 cells were transduced with a lentiviral vector carrying a small hairpin RNA targeting *Nfix* (sh*Nfix*) or a scrambled sequence as a control (scramble). The transduction effectively resulted in the downregulation of *Nfix* expression in sh*Nfix*-treated C2C12, as confirmed by western blot (Figure 5B). Importantly, Myostatin expression was upregulated in *Nfix*-silenced myotubes starting from day 5, confirming that *Nfix* was able to downregulate Myostatin expression in differentiating C2C12 myoblasts (Figure 5C).

*Nfix* can bind with high affinity to the palindromic consensus sequence TTGGC(N5)GCCAA (Kruse and Sippel, 1994), although NFI factors can also bind to hemi-binding sites (a single TTGGC or GCCAA site alone) (Gronostajski, 2000) with a lower affinity. In silico analysis using Genomatix Software allowed us to identify hypothetical *Nfix* hemi-binding sites in the Myostatin

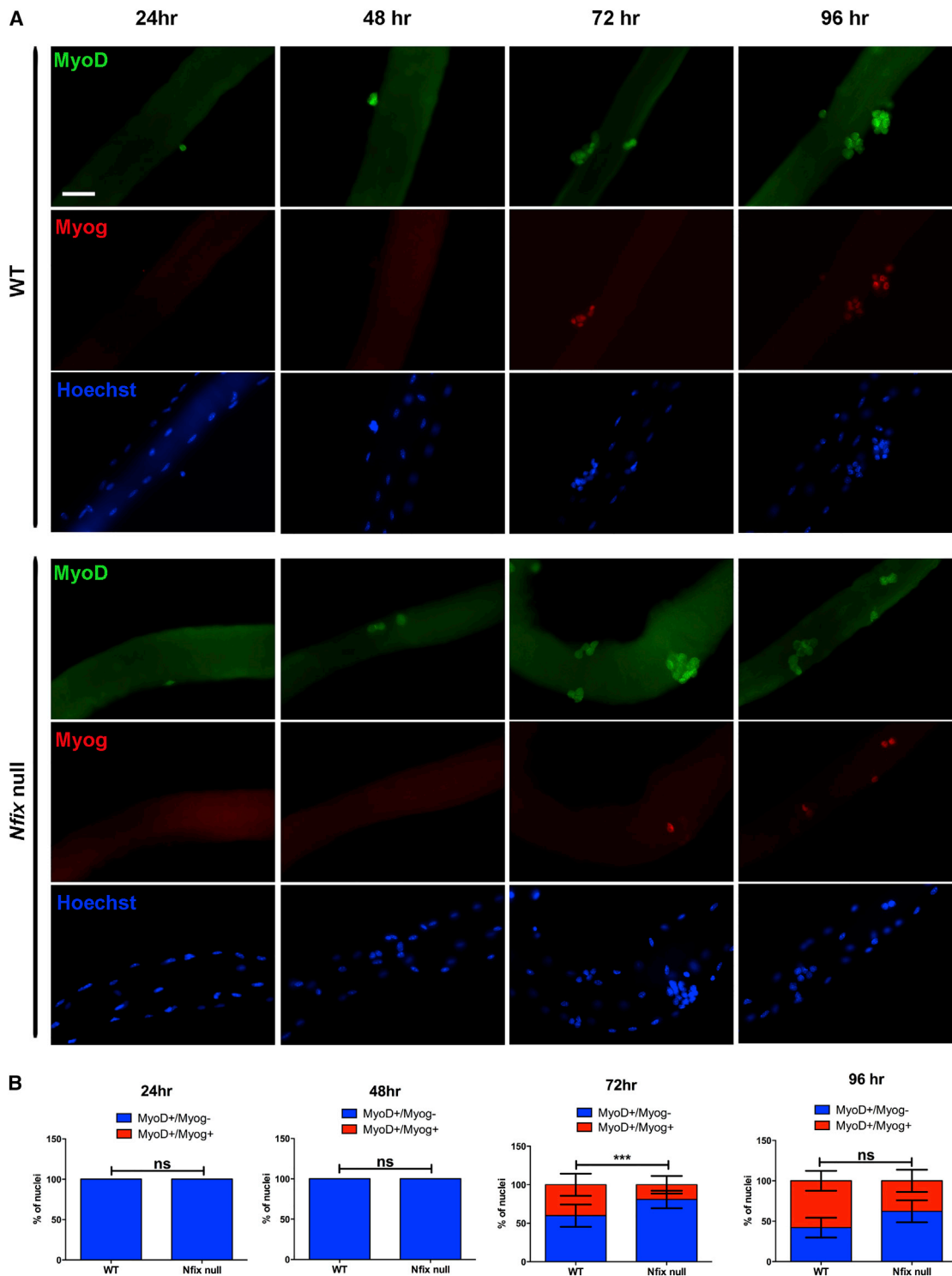


**Figure 2. SCs Lacking Nfix Are Characterized by a Delayed Differentiation**

(A) Immunofluorescence analysis of MyoD (green) and Myogenin (Myog, red) expression on single muscle fibers from WT and *Nfix*-null muscles after 24, 48, 72, and 96 hr in culture. Hoechst was used to stain nuclei ( $n = 3$  WT and 3 *Nfix*-null mice). The scale bar represents 50  $\mu\text{m}$ .

(B) Quantification of MyoD<sup>+</sup>/Myogenin<sup>+</sup> and MyoD<sup>+</sup>/Myogenin<sup>-</sup> SCs associated with WT and *Nfix*-null myofibers at 24, 48, 72, and 96 hr in culture. The quantification is the result of three independent experiments on three WT and three *Nfix*-null mice. The data are presented as mean  $\pm$  SD (not significant, ns; \*\*\* $p < 0.001$  with  $n = 11$  WT myofibers and  $n = 16$  *Nfix*-null myofibers; and two-tailed unpaired t test).

See also Figure S2.

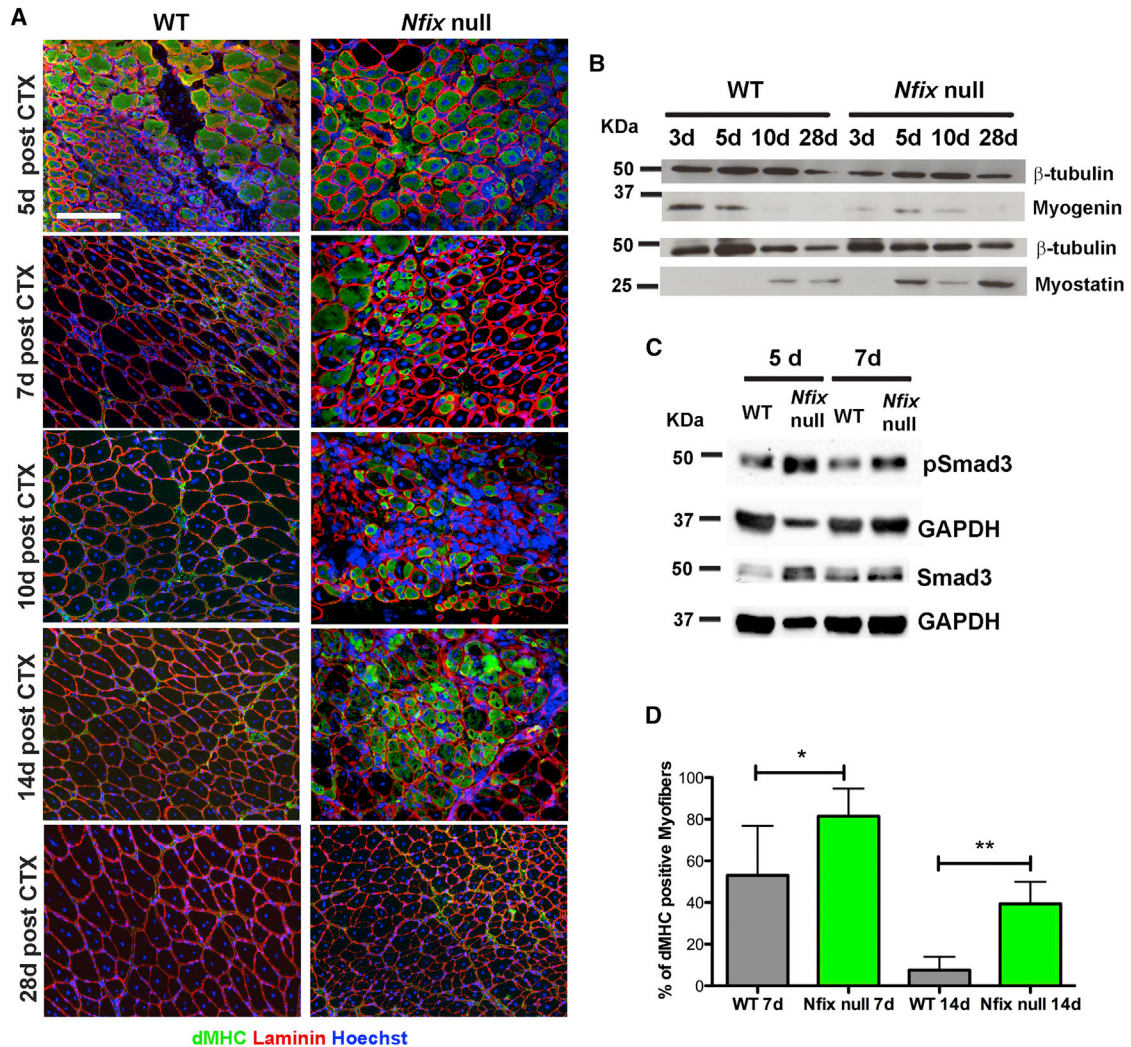


**Figure 3. Absence of *Nfix* Leads to a Marked Impairment of Muscle Regeneration after Injury**

(A) Immunofluorescence for dMHC (green) on regenerating WT and *Nfix*-null *Tibialis anterior* muscles 5, 7, 10, 14, and 28 days (d) following CTX injection. The laminin is marked in red and Hoechst was used to stain nuclei ( $n = 3$  mice for each group). The scale bar represents 50  $\mu$ m.

(B) Western blot analysis of Myogenin and Myostatin expression on WT and *Nfix*-null muscles 3, 5, 10, and 28 days (d) following CTX injection. The  $\beta$ -tubulin was used to normalize.

(C) Western blot analysis of pSmad3 and Smad3 expression on WT and *Nfix*-null muscles 5 and 7 days (d) following CTX injection. GAPDH was used to normalize.

(D) Quantification of the percentage of dMHC positive myofibers in WT and *Nfix*-null mice after 7 and 14 days following CTX injection ( $n = 6$  mice for time point 7 and  $n = 5$  mice for time point 14). The data are presented as mean  $\pm$  SD (\* $p < 0.05$ ; \*\* $p < 0.01$ ; and two-tailed unpaired t test).

See also Figure S2E.

promoter that were used to design specific primers. Notably, the identified sites are flanked by putative binding sites for MEF-2, which is a known co-factor of *Nfix* (Messina et al., 2010).

To assess whether *Nfix* can bind directly and regulate the Myostatin promoter, we performed a chromatin immunoprecipitation (ChIP) assay on differentiating C2C12. Proliferating C2C12 myoblasts were transduced with a HA-tagged *Nfix2* lentiviral vector and then ChIP analysis was performed after 4 days in differentiation medium on the identified *Nfix* binding domains of Myostatin promoter. As expected, *Nfix* bound to the *Nfatc4* promoter as described previously (Messina et al., 2010), and it was also found to directly bind to Myostatin promoter (Figure 5D). To

determine how *Nfix* binding affected Myostatin expression, we transduced wild-type and *Nfix*-null SC-derived myoblasts with a *Nfix2*-HA lentivirus. A significant decrease in Myostatin expression was noted following *Nfix* overexpression, both in wild-type and in *Nfix*-null myoblasts (Figure 5E), thereby confirming the repressive role of *Nfix* on *Mstn* expression.

#### In Vivo Silencing of Myostatin Rescues the Regeneration Delay in *Nfix*-Null Mice

From the results indicated above, we predicted that regeneration defects observed in *Nfix*-null mice would be rescued by reducing Myostatin expression. Due to lethality of perinatal mice and

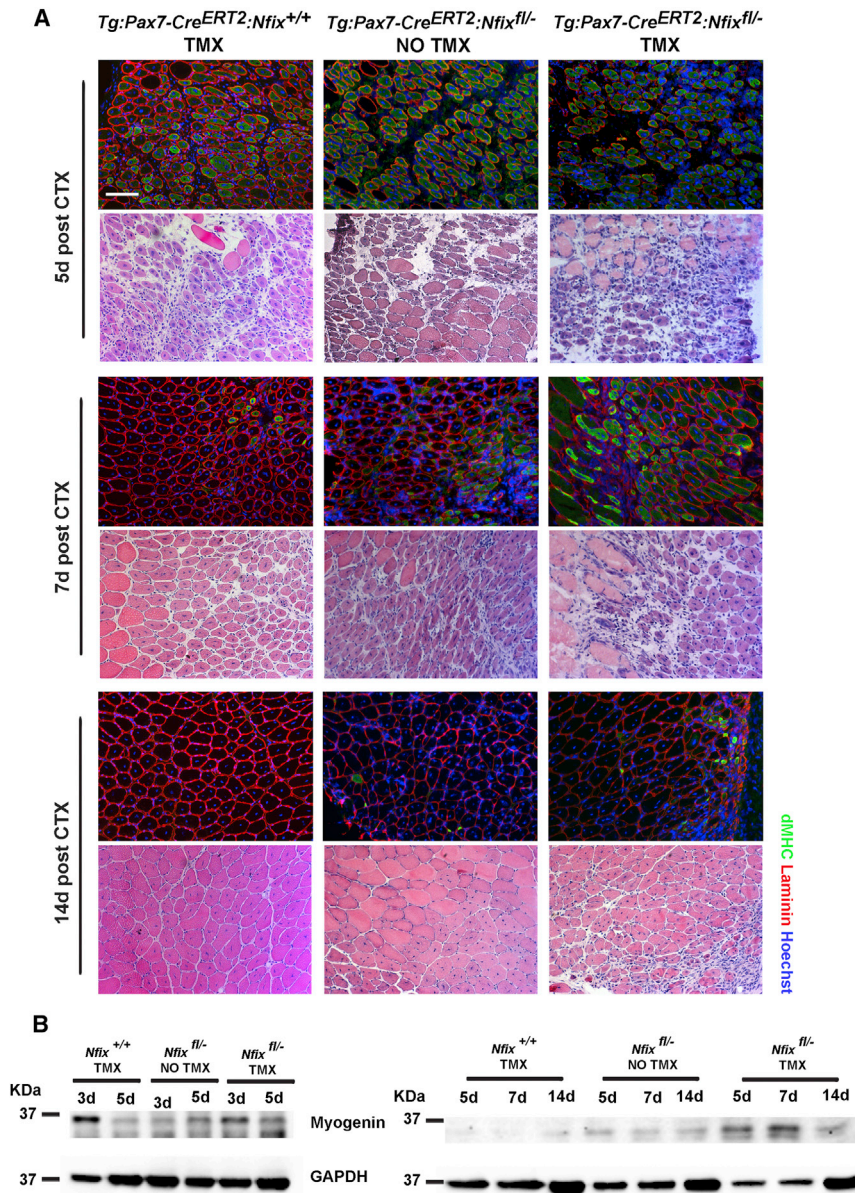


**Figure 4. Absence of Nfix in SCs Determines the Delay in Muscle Regeneration**

(A) H&E staining and immunofluorescence for dMHC (green) on transverse sections of regenerating *Tibialis anterior* muscles from *Tg:Pax7-Cre<sup>ERT2</sup>:Nfix<sup>+/+</sup>* and *Tg:Pax7-Cre<sup>ERT2</sup>:Nfix<sup>fl/-</sup>* mice with (TMX) or without (NO TMX) tamoxifen treatment. The muscles were collected and stained after 5, 7, and 14 days (d) from CTX injection. The laminin is marked in red and Hoechst was used to stain nuclei (n = 3 mice for each group). The scale bar represents 100  $\mu$ m.

(B) Western blot analysis of Myogenin expression on regenerating muscles from *Tg:Pax7-Cre<sup>ERT2</sup>:Nfix<sup>+/+</sup>* (*Nfix<sup>+/+</sup>*) and *Tg:Pax7-Cre<sup>ERT2</sup>:Nfix<sup>fl/-</sup>* mice (*Nfix<sup>fl/-</sup>*) with (TMX) or without (NO TMX) tamoxifen treatment after 3, 5, 7, and 14 days (d) from CTX injection. Myogenin and GAPDH in the right panel come from two separate gels but using the same samples and protein amount. GAPDH was used to normalize. See also Figure S3.

difficulties in obtaining viable *Nfix:Mstn* double-null mice, we electroporated wild-type and *Nfix*-null regenerating *Tibialis anterior* muscles with control plasmids (scramble) or plasmids carrying an shRNA targeting *Mstn* (*shmstn*). Initial studies were carried out to verify the correct downregulation of *Mstn* expression after electroporation of the *shmstn* plasmid both in entire muscles and in re-isolated myoblasts (Figures S4A and 6C). We then electroporated scramble and *shmstn* plasmids 4 days after muscle injury, to obtain the maximal downregulation of Myostatin around day 6, which corresponds to the temporal window in which Myostatin was upregulated in *Nfix*-null mice (Figure 3B). Muscles were then isolated and processed at different time points after injury. Remarkably, we obtained a rescue of the regeneration defects of *Nfix*-null mice in muscles treated with the *shmstn* plasmid, but not with the scramble control vec-

tor (Figure 6A). This was particularly evident at 14 days after muscle injury, as shown by analysis of muscle sections stained for dMHC. The differences observed were even more striking in total muscle section reconstructions (Figure S4C). The analysis of the cross sectional area of regenerating myofibers revealed, as expected, a reduced cross sectional area for *Nfix*-null muscles with respect to wild-type. However, the regenerative delay phenotype was rescued upon Myostatin silencing; *shmstn* treated *Nfix*-null myofibers were comparable in size to scramble-treated wild-type (WT) fibers at the same time points (Figure S4B). This result highlights Myostatin involvement in the regeneration defects of *Nfix*-null mice, although from this experiment we cannot rule out the contribution of Myostatin to *Nfix*-null myofiber

size in resting conditions. Strikingly, the regeneration rescue is supported by quantification of dMHC, whose expression was significantly reduced as a consequence of Myostatin silencing in *Nfix*-null mice (Figure 6B).

## DISCUSSION

Developmental and regenerative myogenesis share common and distinct features. Previous work from our group demonstrated that *Nfix* is responsible for the transcriptional switch from embryonic to fetal myogenesis during prenatal development (Messina et al., 2010). In the present study, we show that *Nfix* is required for maintaining muscle physiology postnatally and for the proper timing of muscle regeneration, where we report a link between *Nfix* and *Mstn* expression. Notably, the

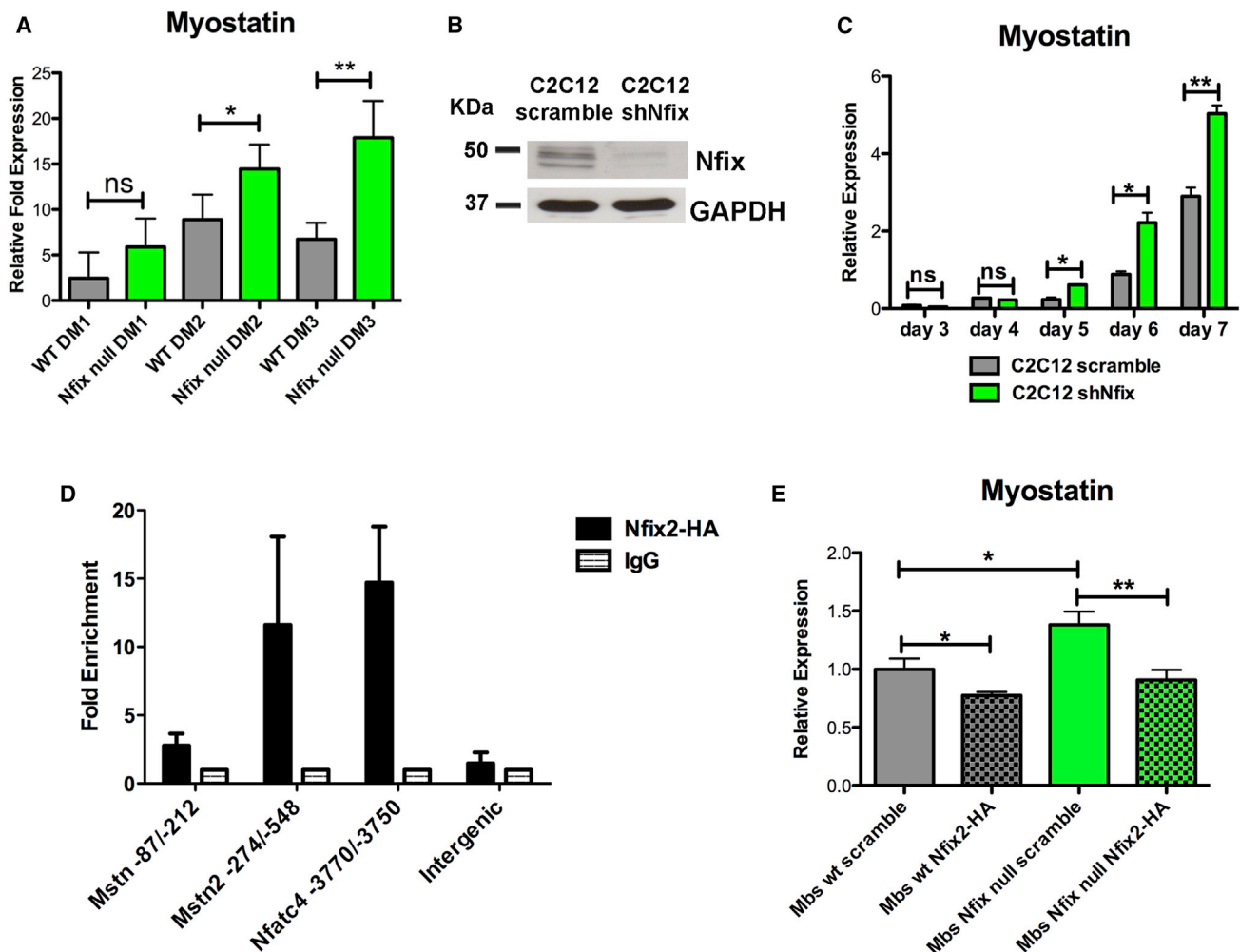


**Figure 5. Nfix Regulates Myostatin Expression in Differentiating Myoblasts through a Direct Binding to its Promoter**

(A) Real-time qPCR showing Myostatin upregulation in differentiating SC-derived myoblasts. The SCs were isolated by FACS and plated in differentiation medium for a time course analysis from 1 to 3 days (DM1, DM2, and DM3) (n = 4 DM1 WT, n = 2 DM1 *Nfix*-null, n = 5 DM2 WT, n = 3 DM2 *Nfix*-null, n = 4 DM3 WT, and n = 4 DM3 *Nfix*-null). The data are presented as mean  $\pm$  SD (not significant, ns; \*p < 0.05; \*\*p < 0.01; and two-tailed unpaired t test).

(B) Western blot analysis of Nfix expression in C2C12 myoblasts transduced with a control vector (C2C12 scramble) or with a vector carrying a shRNA targeting Nfix (C2C12 shNfix). GAPDH was used to normalize.

(C) Real-time qPCR analysis of Myostatin expression in scramble and shNfix C2C12 in a time course from 3 to 7 days in differentiation medium. The values are plotted as relative expression and normalized to GAPDH (n = 3 independent samples for each time point). The data are presented as mean  $\pm$  SD (not significant, ns; \*p < 0.05; \*\*p < 0.01; and two-tailed unpaired t test).

(D) ChIP on differentiated C2C12 transduced with a vector expressing a HA-tagged Nfix2 isoform to test binding to putative Nfix binding sites on Myostatin promoter located at  $-87/-212$  bp and  $-274/-548$  bp from transcription start site. Binding on *Nfatc4* promoter and on an intergenic region were used as positive and negative controls, respectively. The data are means of two independent experiments and expressed as fold enrichment (mean  $\pm$  SD) relative to the IgG signal (n = 3 independent ChIP).

(E) Real-time qPCR for Myostatin in WT and *Nfix*-null SC-derived myoblasts transduced with a control vector (scramble) or with a vector overexpressing the Nfix2 isoform (Nfix2-HA). The values are plotted as relative expression and normalized to GAPDH (n = 3 samples for each group). The data are presented as mean  $\pm$  SD (\*p < 0.05; \*\*p < 0.01; and two-tailed unpaired t test).

absence of Nfix leads to a dramatic delay in muscle regeneration *in vivo*, and this phenotype can be rescued by suppressing *Mstn* expression.

One of the main features that we observed in *Nfix*-null muscles was an altered muscular physiology characterized by a strikingly reduced muscle fiber size and an overexpression of the slow MyHC isoform. As already observed during prenatal develop-

ment, the ability of Nfix to modulate slow MyHC expression is maintained after birth. Since Nfix plays important roles in brain and CNS development (Campbell et al., 2008), those phenotypes might directly or indirectly impact on the muscle phenotypes reported here. However, we show that upregulation of slow MyHC in the absence of Nfix is reproducible in SC-derived myotubes in culture, thus suggesting that the phenotype

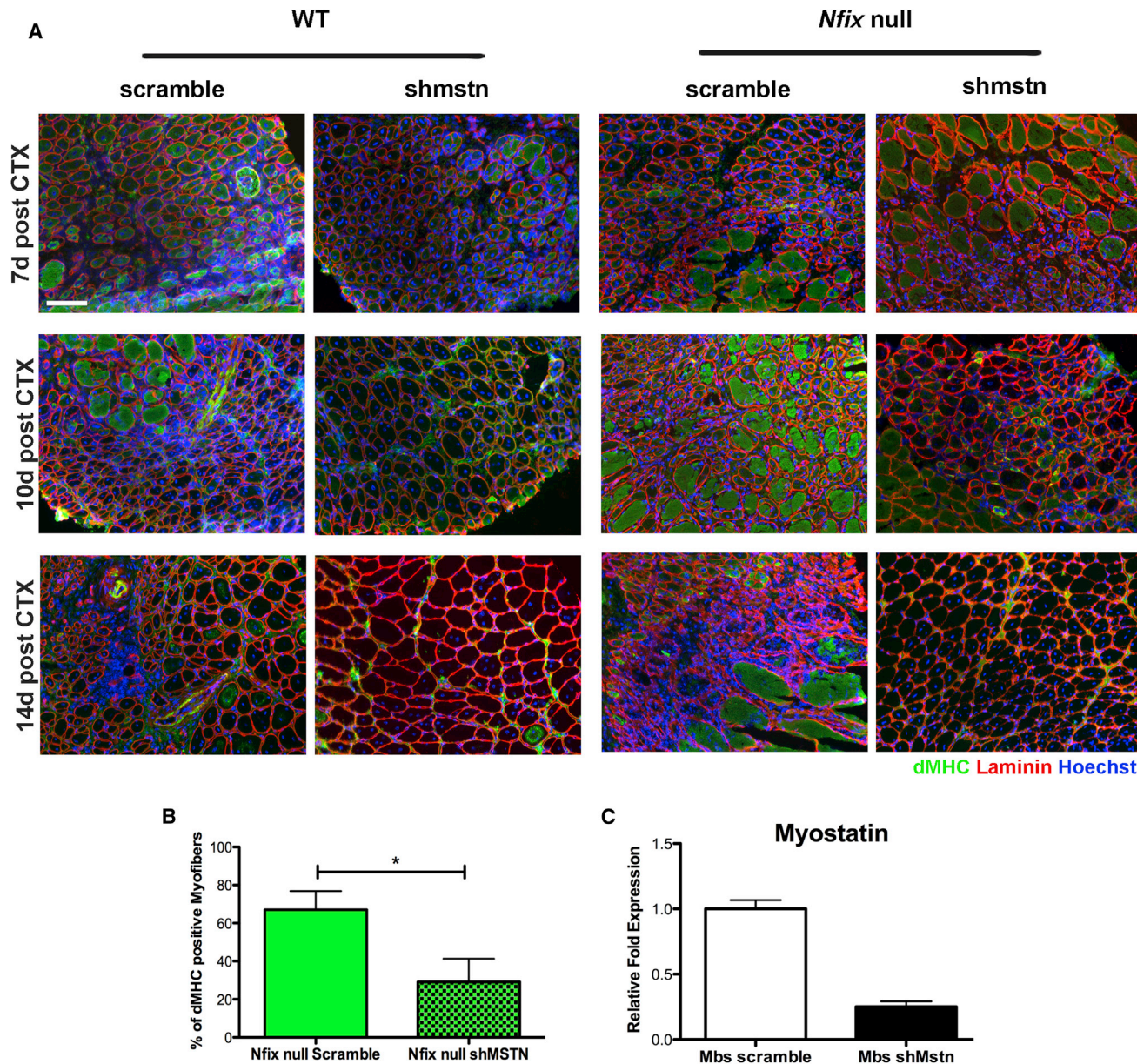


**Figure 6. In Vivo Silencing of Myostatin in Regenerating *Nfix* Null Muscles Rescues their Regeneration Defects**

(A) Immunofluorescence analysis of dMHC expression (green) on regenerating WT and *Nfix*-null *Tibialis anterior* muscles after muscle electroporation with a control plasmid (scramble) or with a plasmid carrying an shRNA targeting Myostatin (shmstn). The muscles were electroporated after 4 days following CTX injection and were collected and stained after 7, 10, and 14 days (d) following CTX injection. The laminin is marked in red and Hoechst was used to stain nuclei ( $n = 3$  mice for each group). The scale bar represents 100  $\mu\text{m}$ .

(B) Quantification of the percentage of dMHC positive myofibers in *Nfix*-null mice electroporated with scramble or shmstn plasmids after 7 and 14 days following CTX injection ( $n = 5$  mice for each group). The data are presented as mean  $\pm$  SD ( $*p < 0.05$  and two-tailed unpaired t test).

(C) Real-time qPCR showing Myostatin expression in myoblasts re-isolated from *Tibialis anterior* electroporated with control (scramble) or shMyostatin (shMstn) plasmids. The myoblasts were isolated the day after in vivo transfection, and cultures were stopped 2 days later to perform qRT-PCR. The data are presented as mean  $\pm$  SD.

See also Figure S4.

observed is cell-autonomously dependent on *Nfix* function in muscle. Moreover, ChIP experiments on C2C12 confirmed *Nfix* binding to *Nfatc4* promoter, further suggesting that the mechanism of action is conserved between prenatal and postnatal life.

We also noted delayed differentiation of single fiber-associated myogenic cells that is accompanied by the modulation of *Myogenin* expression. This finding is consistent with the marked delay in regeneration observed in *Nfix*-null mice.

Importantly, in addition to the persistent expression of dMyHC and to a delayed expression of *Myogenin* we observed a sustained expression of *Mstn* in injured muscles of *Nfix*-null mice. Myostatin (GDF8) is a potent inhibitor of myogenesis, where a dramatic increase in muscle mass was reported in *Mstn*-null mice (McPherron et al., 1997). However, the mode of action of Myostatin remains under debate for both prenatal and postnatal myogenesis (Manceau et al., 2008). Here, we show that the increased expression of *Mstn* in both *Nfix* silenced differentiating C2C12 cells and SC-derived myoblasts, as also in *Nfix*-null regenerating muscles, correlates with the delayed differentiation in vitro and in injured muscles. Myostatin is known to inhibit myoblast differentiation through inhibition of SC activation and proliferation (McCroskery et al., 2003; Taylor et al., 2001) and through repression of MyoD activity (Langley et al., 2002). Moreover, inhibition of Myostatin is known to accelerate muscle regeneration (McCroskery et al., 2005), thus supporting a causative relationship between the increase in Myostatin levels that we observed in regenerating *Nfix*-null mice and the delayed regeneration that characterizes them. We note that differences between WT and *Nfix*-null mice are apparent in muscles from day 5 after CTX injection, coinciding with the first difference in *Mstn* expression. Moreover, in vivo silencing of *Mstn* in adult *Nfix*-null muscles resulted in recovery of the correct timing of muscle regeneration after injury, confirming the causative relationship between *Mstn* sustained expression and the delayed regeneration observed in mice lacking *Nfix*. Importantly, the delayed regeneration was observed also in tamoxifen treated *Tg:Pax7-Cre<sup>ERT2</sup>:Nfix<sup>fl/-</sup>* mice, supporting the central role played by *Nfix* in SCs. Accordingly, isolated SC-derived *Nfix*-null myotubes express higher levels of Myostatin during differentiation and this is reversed upon *Nfix* re-expression. We therefore identified a mechanism of action for *Nfix* by showing that it can act as a direct regulator of *Mstn*. In light of contradictory reports on the mode of action of Myostatin, it is important to underscore the potentially distinct contextual roles of Myostatin (Manceau et al., 2008). Similar to the contextual roles of Notch signaling in adult myogenesis (Mourikis et al., 2012a, 2012b; Rios et al., 2011), recent studies suggest that Myostatin is necessary to regulate to proper balance between proliferation and differentiation of progenitor cells (George et al., 2013; Manceau et al., 2008; McCroskery et al., 2003).

Here, we suggest that *Mstn* regulation is temporally controlled for appropriate muscle differentiation and regeneration. Forced *Mstn* expression or silencing would inevitably led to a complete block in regeneration or to an accelerated differentiation at the expense of the proper muscle physiology.

In summary, this work demonstrates that *Nfix* acts through an inhibitory mechanism at the *Mstn* promoter in differentiating myoblasts, thereby influencing the commitment of SCs during differentiation and the proper timing of muscle regeneration. The mechanism identified not only broadens our knowledge on the function of *Nfix* in postnatal skeletal myogenesis, but also contributes to our understanding of molecular mechanisms involved in the regulation of *Mstn*.

## EXPERIMENTAL PROCEDURES

### Animal Models

*Nfix*-null mice were generated crossing heterozygous mice obtained from Prof. Richard M. Gronostajski (University of Buffalo) and were always compared to WT littermates or age-matched WT mice. To increase *Nfix*-null mice survival, their food was supplemented with a soft dough chow (Transgenic Dough Diet, Bioserv) starting from postnatal day (P)21, as described (Campbell et al., 2008). WT mice used as controls were fed with the same diet. *Tg:Pax7-Cre<sup>ERT2</sup>* mice were described previously (Mourikis et al., 2012b). *Nfix<sup>fl</sup>* mice were obtained from Prof. Richard M. Gronostajski (Campbell et al., 2008). Mouse genotyping was performed by PCR (GoTaq DNA Polymerase, Promega) using the primers listed in Table S1. For muscle regeneration, 20  $\mu$ l of 100  $\mu$ M CTX from *Naja mossaibica* (Sigma-Aldrich) were injected in the *Tibialis anterior* of 2-month-old mice. Induction of *Nfix* deletion in *Tg:Pax7-Cre<sup>ERT2</sup>:Nfix<sup>fl/-</sup>* was performed by multiple tamoxifen injections. Starting from P18, mice received three subcutaneous injections (one every 24 hr for 3 days) of 50  $\mu$ g tamoxifen (20 mg/ml) per gram of mouse. At 1 week before CTX, mice were subjected to an intraperitoneal injection of 25 mg/ml tamoxifen (250  $\mu$ g per gram of mouse). Starting from the day after, mice were fed with a specific tamoxifen enriched or control diet (Harlan). A detailed scheme of tamoxifen treatment is described in Figure S3A.

Mice were kept in pathogen-free conditions and all procedures were conformed to Italian law (D. Lgs n° 2014/26, implementation of the 2010/63/UE) and approved by the University of Milan Animal Welfare Body and by the Italian Minister of Health.

### Measurement of Myofiber Cross Sectional Area

Cross sectional area of the myofibers was calculated on section images obtained from *Tibialis anterior* muscles using ImageJ.

### Cell Culture

C2C12 cells (ATCC) were cultured at 37°C, 5% CO<sub>2</sub> in DMEM (Lonza) plus 20% fetal bovine serum (FBS) (Lonza), 2 mM L-Glutamine (Sigma-Aldrich), and 1% Penicillin/Streptomycin (Euroclone). Differentiation was induced plating 1.5  $\times$  10<sup>5</sup> cells in 35 mm petri dishes with DMEM, 2% horse serum (Lonza), 2 mM L-Glutamine and 1% Penicillin/Streptomycin.

### SC Isolation and Culture

SCs (myoblasts) were isolated from WT and *Nfix*-null mice at P7–P10. Forelimb, hindlimb, and diaphragm muscles were dissected, mechanically cut, and enzymatically digested at 37°C under constant shaking with a solution containing Collagenase I (100  $\mu$ g/ml, Sigma-Aldrich), Dispase (500  $\mu$ g/ml, Gibco), and DNaseI (100  $\mu$ g/ml, Roche) in PBS (Sigma-Aldrich). Undigested tissue was precipitated for 5 min, and the supernatant was centrifuged for 5 min at 1,200 g. The cell pellet was resuspended in DMEM plus 10% FBS, 3% chick embryo extract, 2 mM L-Glutamine, 1% Penicillin/Streptomycin and preplated in 150 mm petri dishes for 1 hr. After pre-plating, the non-adherent, myoblast enriched population was collected and plated in collagen coated (Collagen from calf skin, Sigma-Aldrich) 90 mm petri dishes at a density of 15,000 cells per petri. After a few days in proliferation, the myoblasts were eventually plated at high density (250,000 cells in 35 mm dishes) in differentiation medium (DMEM, 5% horse serum, 2 mM L-Glutamine, and 1% Penicillin/Streptomycin).

For cell sorting experiments, tissues were processed similarly, and then cells were blocked with 10% donkey serum (Sigma-Aldrich) in PBS for 15 min at room temperature (RT). The cells were incubated 30 min on ice with primary antibody detecting SM/C-2.6 antigen, biotinylated, 1:200 (Fukada et al., 2004). After two washes, cells were incubated with Streptavidin-APC (BD Pharmingen, 1:500) and CD45-FITC (Rat Anti-Mouse, 30-F11, BD Pharmingen, 1:100), 20 min on ice. The cells were washed again and sorted with a MoFlo XDP cell sorter (Beckman Coulter) based on positivity for SM/C-2.6 antigen and negativity for CD45.

### BrdU Incorporation

For BrdU incorporation, 3  $\times$  10<sup>4</sup> SC-derived myoblasts were plated in 35 mm petri dishes. The cells were exposed for 1 hr to 50  $\mu$ M BrdU (Amersham). The

cells were then fixed with 95% EtOH-5% acetic acid (VWR) for 20 min at RT, incubated with PBS-1.5 M HCl (VWR) for 10 min at RT, washed twice with PBS, and permeabilized with 0.2% Triton in PBS. Primary antibody (1:100, anti-Bromo-deoxyuridine clone BU-1, Amersham) was incubated for 1 hr at 4°C. After four washes, secondary antibody (1:500) was incubated with Hoechst for 40 min at RT. The cells were washed twice with PBS before mounting.

### ELISA Assay for Caspase 9 Concentration

Measurement of the apoptosis rate was performed with an ELISA kit for the detection of mouse Caspase-9 concentration (Cusabio Biotech), according to manufacturer's instructions. Data were acquired with a spectrophotometer (wavelength 450 nm, Tecan). Calculation of results was performed using Curve Expert software.

### Single Fiber Isolation and Culture

Single muscle fibers were isolated from gastrocnemius and quadriceps muscles as previously described (Rosenblatt et al., 1995). In brief, muscles were enzymatically dissociated with 0.2% Collagenase I (Sigma-Aldrich) in DMEM for 30 min at 37°C with constant rolling. Single fibers were isolated under a stereomicroscope by gently passing through fire-polished Pasteur pipettes with different sized apertures. Purified single fibers were transferred in new plates with SC growth medium, cultured at 37°C, 5% CO<sub>2</sub>, and fixed for staining with 4% paraformaldehyde every 24 hr from 0 to 96 hr. EdU incorporation and staining were performed using the Click-iT EdU Alexa Fluor 594 Imaging Kit (Life Technologies), according to manufacturer's instruction.

### Lentiviral Transduction

C2C12 myoblasts were transduced with a lentivirus carrying a scrambled sequence or a shNfix. Transduction was performed in suspension (in DMEM 20% FBS), at a MOI of 100 and in the presence of Polybrene (8 µg/ml, Sigma-Aldrich). After overnight (O/N) incubation, the medium was changed, and cells were treated with puromycin (2 µg/ml, Sigma-Aldrich). SC-derived myoblasts and C2C12 used for ChIP experiments were transduced with a lentiviral vector carrying a control sequence or a Nfix2-HA-tagged isoform, described in Messina et al. (2010).

### Immunofluorescence and Histology

Muscles were isolated from tendon to tendon, rapidly passed in liquid nitrogen-cooled isopentane (VWR) for 1 min, then in liquid nitrogen for 2 min, and left at -80°C until processed. There were 7 µm sections that were cut with a cryostat (Leica) on positively charged glass slides (Superfrost Plus, Thermo Scientific). Muscle sections were stained with H&E (Sigma-Aldrich) according to standard protocols. For immunofluorescence analysis, cells or sections were fixed for 10 min with 4% paraformaldehyde in PBS at 4°C (apart from staining for dMHC that do not require fixation). Samples were then permeabilized with 1% BSA (Sigma-Aldrich)-0.2% Triton X-100 (Sigma-Aldrich) in PBS for 30 min and blocked with 10% goat serum (Sigma-Aldrich) in PBS for 30 min at RT. Primary antibodies were incubated O/N at 4°C in PBS. After two washes with PBS-1% BSA-0.2% Triton, samples were incubated with secondary antibodies (1:500, Jackson Laboratory. Fluorochromes used: 488, 649, 594, and 546) and Hoechst (1:500, Sigma-Aldrich) in PBS for 45 min at RT, washed twice with PBS-0.2% Triton and mounted with Fluorescence Mounting Medium (Dako).

Immunofluorescences on single fibers were performed in suspension. Single myofibers were collected in 1.5 ml tubes and fixed for 10 min with 4% paraformaldehyde in PBS at 4°C. Fixed myofibers were treated with PBS-1% Triton-10% goat serum for 30 min at RT. Primary antibodies were incubated O/N in PBS-1% goat serum. After two washes with a solution containing 1% BSA in PBS, single myofibers were incubated with secondary antibodies and Hoechst in PBS for 1 hr at RT, washed twice with PBS-1% BSA, and mounted on slides.

Images were acquired at RT using a Leica-DMI6000B fluorescence microscope equipped with 10× and 20× magnification objectives. Leica DFC365FX or DFC400 cameras were used for image capture. The Leica Application Suite software was used for acquisition. Single channel pictures were merged using Photoshop. The following primary antibodies and dilutions were used: rabbit

anti-Nfix (1:200, Novus Biologicals); chicken anti-laminin (1:500, Abcam); rabbit anti-laminin (1:300, Sigma-Aldrich); mouse anti Pax7 (1:2, DSHB); mouse anti-total MyHC (MF20) (1:2, DSHB); chicken anti-β-gal (1:500, Abcam); mouse anti-dMHC, which detects the Myh3 isoform (1:40, Monosan); rabbit anti-MyoD (C-20) (1:60, Santa Cruz Biotechnology); and mouse anti-Myogenin (1:3, DSHB).

### RNA Extraction, RT-, and Real-Time qPCR

Total RNA from cultured cells was extracted using the NucleoSpin kits RNA XS and II (Macherey-Nagel). Isolation of total RNA from muscles was performed with TRIzol Reagent (Invitrogen) according to the manufacturer's instructions. RNA was quantified using a NanoPhotometer (Implen). There was 1 µg of total RNA for each sample that was retrotranscribed with the iScript Reverse Transcription Supermix for RT-quantitative (q)PCR (Bio-Rad) in a total volume of 20 µl. For qRT PCR, cDNA was diluted 1:10 and 5 µl of the diluted cDNA was loaded in a total volume of 20 µl (iQaq Universal, Bio-Rad). Primers used are listed in Table S2. The relative quantification of gene expression was determined by comparative CT method, and normalized to glyceraldehyde 3-phosphate dehydrogenase (GAPDH).

### ChIP Assay

For ChIP, 3.5 × 10<sup>6</sup> scramble C2C12 myoblasts per antibody were plated. The cells were maintained in culture for 1 day in DMEM, 20% FBS, and then induced to differentiate with DMEM, 2% horse serum, at a density of 1.5 × 10<sup>6</sup> cells in 90 mm petri dishes. Crosslink was performed at day 4 in differentiation with 1% formaldehyde (Sigma-Aldrich) in DMEM for 10 min. Crosslink was blocked with 0.125 M Glycine (Sigma-Aldrich) in PBS for 10 min while shaking. After two washes with PBS, cells were scraped with PBS containing protease inhibitors and phenylmethanesulfonyl fluoride (PMSF) and centrifuged for 15 min at 1,500 g at 4°C. The cell pellet was dounced 20 times in a 7 ml pestle in swelling buffer, then centrifuged for 10 min at 5,000 g at 4°C, and the nuclei pellet was sonicated with a Bioruptor Sonicator (Diagenode) for 15 min, with repeated cycles of 15 s of sonication and 15 s of resting. Samples were finally centrifuged for 10 min at 12,000 g at 4°C, and chromatin-enriched supernatant was used in the following passages. Chromatin was pre-cleared for 2 hr with Protein G Sepharose (PrG, 15 µl per sample) (Amersham) and rabbit serum (2.5 µl per sample) and for 2 hr with PrG previously blocked with BSA (10 µg/ml) and Salmon Sperm (1 µg/ml) (Sigma-Aldrich) on a rotating platform at 4°C. Chromatin was then incubated O/N with primary antibodies. The day after, immunocomplexes were precipitated by addition of blocked PrG for 3 hr on rotating platform at 4°C, then centrifuged for 2 min at 12,000 g at 4°C. Samples were then repeatedly washed and the antibody-protein-DNA complexes were eluted twice for 10 min at 65°C. Eluted samples were incubated O/N at 65°C with 10 µg RNase (Sigma-Aldrich) and 200 mM NaCl (Sigma-Aldrich) to reverse crosslinks. Finally, DNA was treated with Proteinase K (Sigma-Aldrich) (20 µg per sample) for 3 hr at 50°C and then extracted with phenol-chloroform. Obtained DNA samples were analyzed with qPCR and results were plotted as fold enrichment with respect to the IgG sample. Primers used are listed in Table S3.

There were 5 µg of the following primary antibodies that were used: rabbit anti-HA-probe (Y-11, Santa Cruz Biotechnology); normal rabbit IgG (Santa Cruz Biotechnology).

### Western Blot

Total protein extracts were obtained from cells or homogenized tissues, lysed with RIPA or Tissue extraction buffer plus protease and phosphatase inhibitors for 30 min on ice. Samples were then centrifuged 10 min at 12,000 × g at 4°C, and the supernatant transferred into a new tube and quantified using the DC Protein Assay (Bio-Rad). There were 30 µg of total protein extracts that were loaded on a 7%–12% SDS (Sigma-Aldrich) acrylamide gel (Sigma-Aldrich) and blotted to a nitrocellulose membrane (Whatman, Protran Nitrocellulose Transfer Membrane). After 1 hr of blocking in milk, primary antibodies were incubated O/N. Blots were then washed and incubated with secondary antibodies (1:10,000, IgG-HRP, Bio-Rad) for 40 min at RT and washed again. Finally, bands were revealed with ECL detection reagent (Amersham) and exposed to an X-ray film (Hyperfilm ECL, Amersham). In some cases, blots were acquired using the Chemidoc software (Bio-Rad).

The following primary antibodies and dilutions were used: rabbit anti-Nfix (1:5,000, Geneka Biotechnology); mouse anti- $\beta$ -tubulin (1:5,000, Covance); mouse anti-slow MyHC (Bad5, 1:2, DSHB); mouse anti-total MyHC (MF20, 1:5, DSHB); mouse anti-Myogenin (IF5D, 1:3, DSHB); rabbit anti-Myostatin (1:500, Millipore); mouse anti-GAPDH (1:5,000, Sigma-Aldrich); rabbit anti-Smad3 (1:1,000, Abcam); rabbit anti-pSmad3 (1:1,000, Abcam).

### In Vivo Electroporation

In vivo electroporation was performed 4 days after CTX injection. WT and *Nfix*-null mice were anesthetized and 40  $\mu$ g of control (scramble, Sigma-Aldrich), or *shmstn* (Sigma-Aldrich) plasmids were injected in a total volume of 20  $\mu$ l in *Tibialis anterior* muscles. Muscles were then immediately electroporated using a pulse generator (ECM 830, BTX) equipped with 5 mm needle electrodes to generate 100 V pulses, with a fixed duration of 20 ms and an interval of 200 ms between the pulses.

### Statistical Analysis

All data are expressed as mean  $\pm$  SD. Data were graphed using GraphPad Prism and analyzed with the two-tailed unpaired Student's *t* test. \**p* < 0.05; \*\**p* < 0.01; \*\*\**p* < 0.001; and confidence intervals 95%, alpha level 0.05.

### SUPPLEMENTAL INFORMATION

Supplemental Information includes four figures and three tables and can be found with this article online at <http://dx.doi.org/10.1016/j.celrep.2016.02.014>.

### AUTHOR CONTRIBUTIONS

Conceptualization, G.R. and G.M.; Methodology, S.A.; Investigation, G.R., S.A., C.B., S.M., and C.V.; Writing – Original Draft, G.R.; Writing – Review & Editing, S.T., G.C., and G.M.; Supervision, G.M.; and Funding Acquisition, G.M.

### ACKNOWLEDGMENTS

We thank G. Maroli for helpful discussion. We are also grateful to M. Magistrini for technical assistance, C. Villa (FRACTAL) for the Cytometry service, P. Mourikis for help with the tamoxifen protocol, F. Relaix and H. Amthor for their help and exchange of animal models, and R. Gronostajski for the kind exchange of information and animal models. G.R. conducted this study as partial fulfillment of her PhD in Cellular and Molecular Biology, San Raffaele University, Milan. This work received funding from the European Community, ERC StG2011 (RegeneratioNfix 280611), and the Italian Ministry of University and Research (MIUR-Futuro in Ricerca 2010).

Received: May 28, 2015

Revised: December 2, 2015

Accepted: January 28, 2016

Published: February 25, 2016

### REFERENCES

- Bachurski, C.J., Kelly, S.E., Glasser, S.W., and Currier, T.A. (1997). Nuclear factor I family members regulate the transcription of surfactant protein-C. *J. Biol. Chem.* 272, 32759–32766.
- Bedford, F.K., Julius, D., and Ingraham, H.A. (1998). Neuronal expression of the 5HT3 serotonin receptor gene requires nuclear factor 1 complexes. *J. Neurosci.* 18, 6186–6194.
- Biressi, S., Molinaro, M., and Cossu, G. (2007a). Cellular heterogeneity during vertebrate skeletal muscle development. *Dev. Biol.* 308, 281–293.
- Biressi, S., Tagliafico, E., Lamorte, G., Monteverde, S., Tenedini, E., Roncaglia, E., Ferrari, S., Ferrari, S., Cusella-De Angelis, M.G., Tajbakhsh, S., and Cossu, G. (2007b). Intrinsic phenotypic diversity of embryonic and fetal myoblasts is revealed by genome-wide gene expression analysis on purified cells. *Dev. Biol.* 304, 633–651.
- Bogdanovich, S., Krag, T.O., Barton, E.R., Morris, L.D., Whittemore, L.A., Ahima, R.S., and Khurana, T.S. (2002). Functional improvement of dystrophic muscle by myostatin blockade. *Nature* 420, 418–421.
- Campbell, C.E., Piper, M., Plachez, C., Yeh, Y.T., Baizer, J.S., Osinski, J.M., Litwack, E.D., Richards, L.J., and Gronostajski, R.M. (2008). The transcription factor *Nfix* is essential for normal brain development. *BMC Dev. Biol.* 8, 52.
- Collins, C.A., Olsen, I., Zammit, P.S., Heslop, L., Petrie, A., Partridge, T.A., and Morgan, J.E. (2005). Stem cell function, self-renewal, and behavioral heterogeneity of cells from the adult muscle satellite cell niche. *Cell* 122, 289–301.
- Darville, M.I., Antoine, I.V., and Rousseau, G.G. (1992). Characterization of an enhancer upstream from the muscle-type promoter of a gene encoding 6-phosphofructo-2-kinase/fructose-2,6-bisphosphatase. *Nucleic Acids Res.* 20, 3575–3583.
- Driller, K., Pagenstecher, A., Uhl, M., Omran, H., Berlis, A., Gründer, A., and Sippel, A.E. (2007). Nuclear factor I X deficiency causes brain malformation and severe skeletal defects. *Mol. Cell. Biol.* 27, 3855–3867.
- Edmondson, D.G., Cheng, T.C., Cserjesi, P., Chakraborty, T., and Olson, E.N. (1992). Analysis of the myogenin promoter reveals an indirect pathway for positive autoregulation mediated by the muscle-specific enhancer factor MEF-2. *Mol. Cell. Biol.* 12, 3665–3677.
- Elliott, B., Renshaw, D., Getting, S., and Mackenzie, R. (2012). The central role of myostatin in skeletal muscle and whole body homeostasis. *Acta Physiol. (Oxf.)* 205, 324–340.
- Fukada, S., Higuchi, S., Segawa, M., Koda, K., Yamamoto, Y., Tsujikawa, K., Kohama, Y., Uezumi, A., Imamura, M., Miyagoe-Suzuki, Y., et al. (2004). Purification and cell-surface marker characterization of quiescent satellite cells from murine skeletal muscle by a novel monoclonal antibody. *Exp. Cell Res.* 296, 245–255.
- Funk, W.D., and Wright, W.E. (1992). Cyclic amplification and selection of targets for multicomponent complexes: myogenin interacts with factors recognizing binding sites for basic helix-loop-helix, nuclear factor 1, myocyte-specific enhancer-binding factor 2, and COMP1 factor. *Proc. Natl. Acad. Sci. USA* 89, 9484–9488.
- George, R.M., Biressi, S., Beres, B.J., Rogers, E., Mulia, A.K., Allen, R.E., Rawls, A., Rando, T.A., and Wilson-Rawls, J. (2013). Numb-deficient satellite cells have regeneration and proliferation defects. *Proc. Natl. Acad. Sci. USA* 110, 18549–18554.
- Gronostajski, R.M. (2000). Roles of the NFI/CTF gene family in transcription and development. *Gene* 249, 31–45.
- Hutcheson, D.A., Zhao, J., Merrell, A., Haldar, M., and Kardon, G. (2009). Embryonic and fetal limb myogenic cells are derived from developmentally distinct progenitors and have different requirements for beta-catenin. *Genes Dev.* 23, 997–1013.
- Jackson, D.A., Rowader, K.E., Stevens, K., Jiang, C., Milos, P., and Zaret, K.S. (1993). Modulation of liver-specific transcription by interactions between hepatocyte nuclear factor 3 and nuclear factor 1 binding DNA in close apposition. *Mol. Cell. Biol.* 13, 2401–2410.
- Johanson, M., Meents, H., Ragge, K., Buchberger, A., Arnold, H.H., and Sandmüller, A. (1999). Transcriptional activation of the myogenin gene by MEF2-mediated recruitment of myf5 is inhibited by adenovirus E1A protein. *Biochem. Biophys. Res. Commun.* 265, 222–232.
- Kruse, U., and Sippel, A.E. (1994). The genes for transcription factor nuclear factor I give rise to corresponding splice variants between vertebrate species. *J. Mol. Biol.* 238, 860–865.
- Langley, B., Thomas, M., Bishop, A., Sharma, M., Gilmour, S., and Kambadur, R. (2002). Myostatin inhibits myoblast differentiation by down-regulating MyoD expression. *J. Biol. Chem.* 277, 49831–49840.
- Lepper, C., Partridge, T.A., and Fan, C.M. (2011). An absolute requirement for Pax7-positive satellite cells in acute injury-induced skeletal muscle regeneration. *Development* 138, 3639–3646.
- Manceau, M., Gros, J., Savage, K., Thomé, V., McPherron, A., Paterson, B., and Marcelle, C. (2008). Myostatin promotes the terminal differentiation of embryonic muscle progenitors. *Genes Dev.* 22, 668–681.

- Mauro, A. (1961). Satellite cell of skeletal muscle fibers. *J. Biophys. Biochem. Cytol.* **9**, 493–495.
- McCarthy, J.J., Mula, J., Miyazaki, M., Erfani, R., Garrison, K., Farooqui, A.B., Srikuea, R., Lawson, B.A., Grimes, B., Keller, C., et al. (2011). Effective fiber hypertrophy in satellite cell-depleted skeletal muscle. *Development* **138**, 3657–3666.
- McCroskery, S., Thomas, M., Maxwell, L., Sharma, M., and Kambadur, R. (2003). Myostatin negatively regulates satellite cell activation and self-renewal. *J. Cell Biol.* **162**, 1135–1147.
- McCroskery, S., Thomas, M., Platt, L., Hennebry, A., Nishimura, T., McLeay, L., Sharma, M., and Kambadur, R. (2005). Improved muscle healing through enhanced regeneration and reduced fibrosis in myostatin-null mice. *J. Cell Sci.* **118**, 3531–3541.
- McPherron, A.C., and Lee, S.J. (1997). Double muscling in cattle due to mutations in the myostatin gene. *Proc. Natl. Acad. Sci. USA* **94**, 12457–12461.
- McPherron, A.C., Lawler, A.M., and Lee, S.J. (1997). Regulation of skeletal muscle mass in mice by a new TGF- $\beta$  superfamily member. *Nature* **387**, 83–90.
- Messina, G., Biressi, S., Monteverde, S., Magli, A., Cassano, M., Perani, L., Roncaglia, E., Tagliafico, E., Starnes, L., Campbell, C.E., et al. (2010). Nfix regulates fetal-specific transcription in developing skeletal muscle. *Cell* **140**, 554–566.
- Mourikis, P., Gopalakrishnan, S., Sambasivan, R., and Tajbakhsh, S. (2012a). Cell-autonomous Notch activity maintains the temporal specification potential of skeletal muscle stem cells. *Development* **139**, 4536–4548.
- Mourikis, P., Sambasivan, R., Castel, D., Rocheteau, P., Bizzarro, V., and Tajbakhsh, S. (2012b). A critical requirement for notch signaling in maintenance of the quiescent skeletal muscle stem cell state. *Stem Cells* **30**, 243–252.
- Murphy, M.M., Lawson, J.A., Mathew, S.J., Hutcheson, D.A., and Kardon, G. (2011). Satellite cells, connective tissue fibroblasts and their interactions are crucial for muscle regeneration. *Development* **138**, 3625–3637.
- Pistocchi, A., Gaudenzi, G., Foglia, E., Monteverde, S., Moreno-Fortuny, A., Pianca, A., Cossu, G., Cotelli, F., and Messina, G. (2013). Conserved and divergent functions of Nfix in skeletal muscle development during vertebrate evolution. *Development* **140**, 1528–1536.
- Relaix, F., and Zammit, P.S. (2012). Satellite cells are essential for skeletal muscle regeneration: the cell on the edge returns centre stage. *Development* **139**, 2845–2856.
- Rios, A.C., Serralbo, O., Salgado, D., and Marcelle, C. (2011). Neural crest regulates myogenesis through the transient activation of NOTCH. *Nature* **473**, 532–535.
- Rosenblatt, J.D., Lunt, A.I., Parry, D.J., and Partridge, T.A. (1995). Culturing satellite cells from living single muscle fiber explants. *In Vitro Cell. Dev. Biol. Anim.* **31**, 773–779.
- Sambasivan, R., Yao, R., Kissenpfennig, A., Van Wittenberghe, L., Paldi, A., Gayraud-Morel, B., Guenou, H., Malissen, B., Tajbakhsh, S., and Galy, A. (2011). Pax7-expressing satellite cells are indispensable for adult skeletal muscle regeneration. *Development* **138**, 3647–3656.
- Sartore, S., Gorza, L., and Schiaffino, S. (1982). Fetal myosin heavy chains in regenerating muscle. *Nature* **298**, 294–296.
- Schiaffino, S., Gorza, L., Dones, I., Cornelio, F., and Sartore, S. (1986). Fetal myosin immunoreactivity in human dystrophic muscle. *Muscle Nerve* **9**, 51–58.
- Schuelke, M., Wagner, K.R., Stolz, L.E., Hübner, C., Riebel, T., Kömen, W., Braun, T., Tobin, J.F., and Lee, S.J. (2004). Myostatin mutation associated with gross muscle hypertrophy in a child. *N. Engl. J. Med.* **350**, 2682–2688.
- Spitz, F., Salminen, M., Demignon, J., Kahn, A., Daegelen, D., and Maire, P. (1997). A combination of MEF3 and NFI proteins activates transcription in a subset of fast-twitch muscles. *Mol. Cell. Biol.* **17**, 656–666.
- Szabó, P., Moitra, J., Rencendorj, A., Rákhely, G., Rauch, T., and Kiss, I. (1995). Identification of a nuclear factor- $\kappa$ B family protein-binding site in the silencer region of the cartilage matrix protein gene. *J. Biol. Chem.* **270**, 10212–10221.
- Taylor, W.E., Bhasin, S., Artaza, J., Byhower, F., Azam, M., Willard, D.H., Jr., Kull, F.C., Jr., and Gonzalez-Cadavid, N. (2001). Myostatin inhibits cell proliferation and protein synthesis in C2C12 muscle cells. *Am. J. Physiol. Endocrinol. Metab.* **280**, E221–E228.
- Thomas, M., Langley, B., Berry, C., Sharma, M., Kirk, S., Bass, J., and Kambadur, R. (2000). Myostatin, a negative regulator of muscle growth, functions by inhibiting myoblast proliferation. *J. Biol. Chem.* **275**, 40235–40243.
- Xu, H., Uno, J.K., Inouye, M., Collins, J.F., and Ghishan, F.K. (2005). NF1 transcriptional factor(s) is required for basal promoter activation of the human intestinal NaPi-IIb cotransporter gene. *Am. J. Physiol. Gastrointest. Liver Physiol.* **288**, G175–G181.

**Cell Reports, Volume 14**

**Supplemental Information**

**Nfix Regulates Temporal Progression of Muscle  
Regeneration through Modulation  
of Myostatin Expression**

**Giuliana Rossi, Stefania Antonini, Chiara Bonfanti, Stefania Monteverde, Chiara Vezzali, Shahragim Tajbakhsh, Giulio Cossu, and Graziella Messina**

Supplemental Information

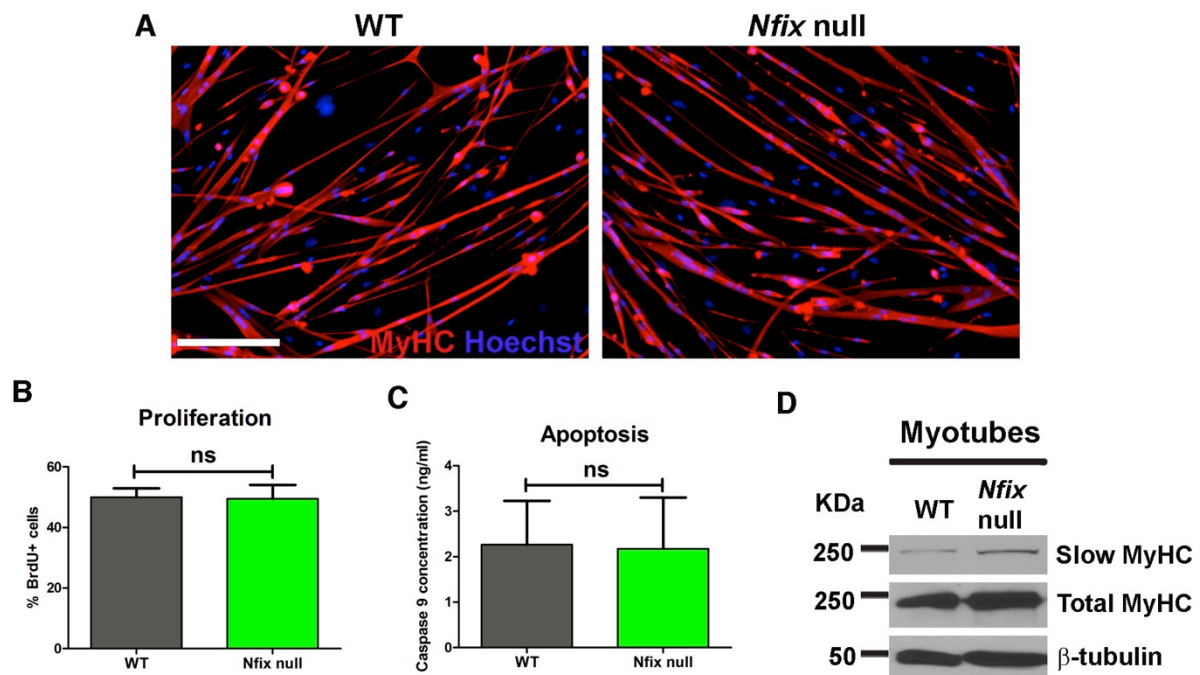


**Fig.S1. Isolated satellite cells in culture correctly differentiate in absence of *Nfix*, while expressing higher levels of slow MyHC, Related to Fig.1.**

(A) Immunofluorescence analysis of total MyHC expression (red) on wild-type and *Nfix* null satellite cell-derived myotubes after 48 h in differentiation medium. Hoechst was used to stain nuclei. n=3 independent myoblast preparations. Scale bar represents 50 $\mu$ m.

(B) Quantification of the percentage of wild-type and *Nfix* null BrdU incorporating myoblasts after 1h of exposure to 50 $\mu$ M BrdU. The experiment was performed in duplicate (n=2 independent myoblast preparations) in proliferation conditions. Data are presented as mean  $\pm$  SD. ns: not significant, two-tailed unpaired *t* Test.

(C) ELISA assay measuring caspase 9 concentration as a marker of apoptosis. The test was performed on protein extracts from wild-type and *Nfix* null proliferating myoblasts. Data are presented as mean  $\pm$  SD. ns: not significant, two-tailed unpaired *t* Test. n=2 assays performed on independent myoblast preparations.

(D) Western blot analysis of slow and total MyHC expression on wild-type and *Nfix* null satellite cell-derived myotubes after 48 h in differentiation medium.  $\beta$ -tubulin was used to normalize the amount of loaded proteins.

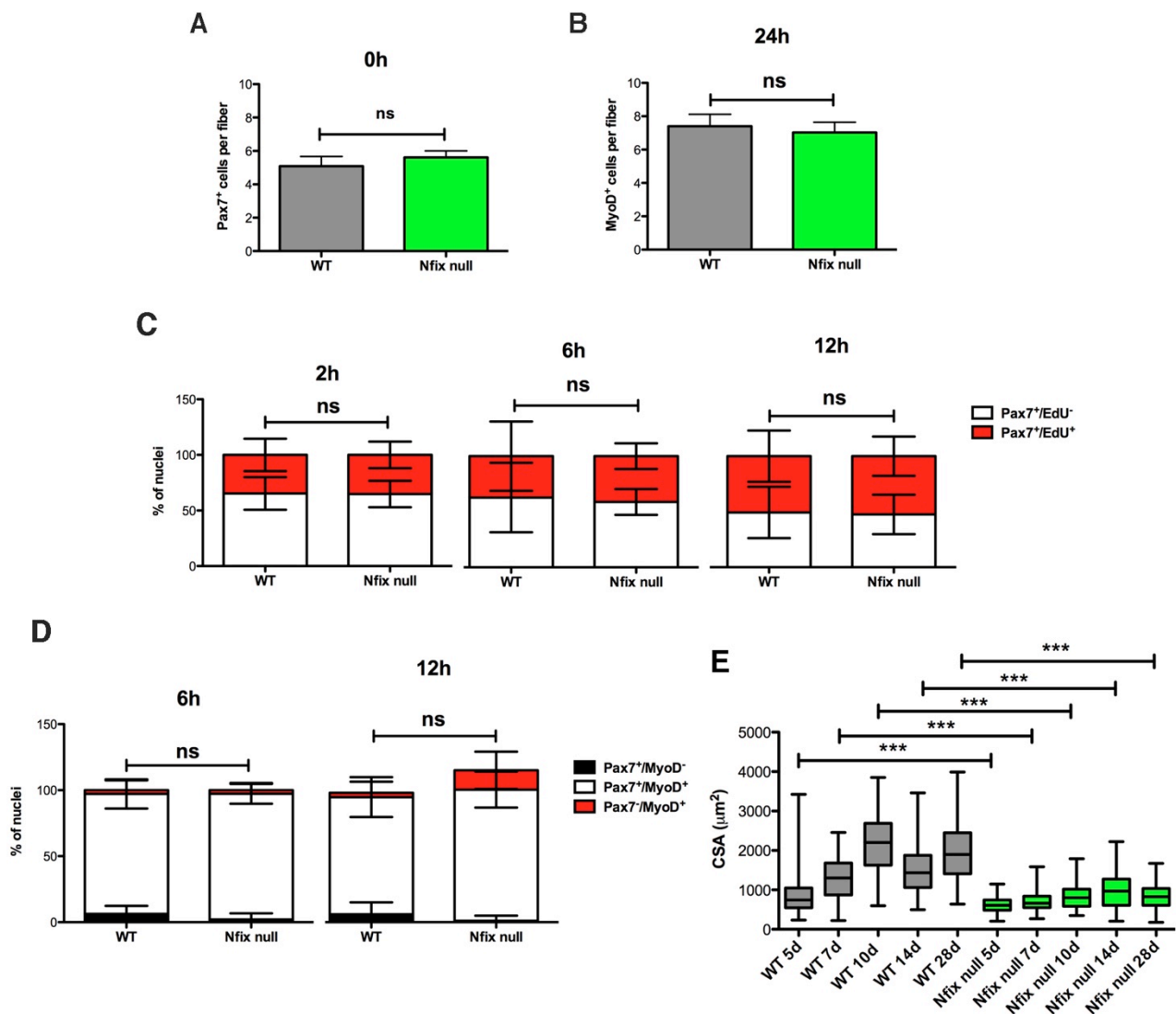


**Fig.S2. Number and proliferation of satellite cells associated to myofibers does not change in the absence of *Nfix*, Related to Figs.2 and 3.**

**(A)** Quantification of Pax7<sup>+</sup> satellite cells associated to freshly isolated wild-type and *Nfix* null myofibers. (n=35 WT and 41 *Nfix* null myofibers). Data are presented as mean ± SD. ns: not significant, two-tailed unpaired *t* Test.

**(B)** Quantification of MyoD<sup>+</sup> satellite cells associated to wild-type and *Nfix* null myofibers after 24 hours in culture. (n=32 WT and 34 *Nfix* null myofibers). Data are presented as mean ± SD. ns: not significant, two-tailed unpaired *t* Test.

**(C)** Quantification of the percentage of proliferating (EdU<sup>+</sup>) wild-type and *Nfix* null satellite cells after 2 (n=18 WT and 14 *Nfix* null myofibers), 6 (n=7 WT and 15 *Nfix* null myofibers), and 12 hours (n=8 WT and 16 *Nfix* null myofibers) (h) in culture. Data are presented as mean ± SD. ns: not significant, two-tailed unpaired *t* Test.

**(D)** Quantification of the percentage of satellite cells expressing MyoD and Pax7 after 6 (n=9 WT and 22 *Nfix* null myofibers) and 12 hours (n=10 WT and 24 *Nfix* null myofibers) in culture. Data are presented as mean ± SD. ns: not significant, two-tailed unpaired *t* Test.

**(E)** Measurement of the myofiber cross sectional area distribution in WT and *Nfix* null regenerating muscles at different time points from injury. n=225 myofibers. Data are presented as mean±whiskers from min to max. \*\*\*P < 0.001; two-tailed unpaired *t* Test.

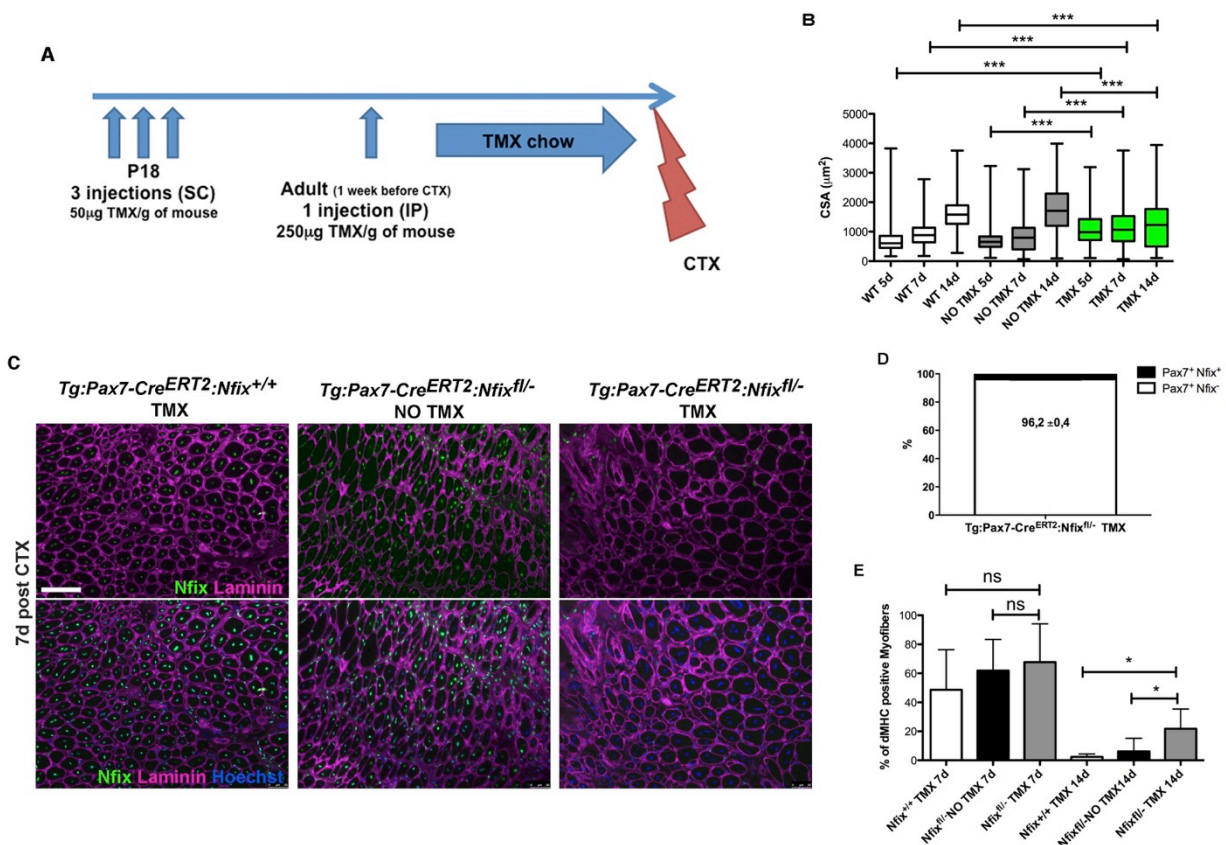


**Fig.S3. Tamoxifen treatment of *Tg:Pax7-Cre<sup>ERT2</sup>:Nfix<sup>fl/-</sup>* mice determines Nfix excision in satellite cells, Related to Fig.4.**

**(A)** Scheme representing the protocol used for tamoxifen treatment (TMX) and cardiotoxin (CTX) injection. SC, subcutaneous. IP, intraperitoneal.

**(B)** Measurement of the myofiber cross sectional area distribution in regenerating muscles of *Tg:Pax7-Cre<sup>ERT2</sup>:Nfix<sup>+/+</sup>* (indicated as WT) and *Tg:Pax7-Cre<sup>ERT2</sup>:Nfix<sup>fl/-</sup>* mice with (TMX) or without (NO TMX) tamoxifen at different time points from injury. n=750 myofibers. Data are presented as mean±whiskers from min to max. \*\*\*P < 0.001; two-tailed unpaired *t* Test.

**(C)** Immunofluorescence analysis of Nfix expression (green) in *Tg:Pax7-Cre<sup>ERT2</sup>:Nfix<sup>+/+</sup>* and *Tg:Pax7-Cre<sup>ERT2</sup>:Nfix<sup>fl/-</sup>* mice with (TMX) or without (NO TMX) tamoxifen treatment 7 days (d) after cardiotoxin injection. Laminin, purple; Hoechst, nuclei. n=3 mice for each group. Scale bar represents 100µm.

**(D)** Graphical representation of the percentage of Nfix excision in tamoxifen treated *Tg:Pax7-Cre<sup>ERT2</sup>:Nfix<sup>fl/-</sup>* mice. Quantification was obtained counting the percentage of cells expressing Pax7 and Nfix in muscle sections. n=2 mice. Data are presented as mean ± SD.

**(E)** Quantification of the percentage of dMHC positive myofibers in *Tg:Pax7-Cre<sup>ERT2</sup>:Nfix<sup>+/+</sup>* and *Tg:Pax7-Cre<sup>ERT2</sup>:Nfix<sup>fl/-</sup>* mice with (TMX) or without (NO TMX) tamoxifen treatment 7 and 14 days following cardiotoxin injection. For time point 7, n=5 *Tg:Pax7-Cre<sup>ERT2</sup>:Nfix<sup>+/+</sup>*, n=8 *Tg:Pax7-Cre<sup>ERT2</sup>:Nfix<sup>fl/-</sup>* NO TMX mice, n=6 *Tg:Pax7-Cre<sup>ERT2</sup>:Nfix<sup>fl/-</sup>* TMX mice. For time point 14, n=5 *Tg:Pax7-Cre<sup>ERT2</sup>:Nfix<sup>+/+</sup>*, n=6 *Tg:Pax7-Cre<sup>ERT2</sup>:Nfix<sup>fl/-</sup>* NO TMX mice, n=6 *Tg:Pax7-Cre<sup>ERT2</sup>:Nfix<sup>fl/-</sup>* TMX mice. Data are presented as mean ± SD. ns: not significant, \*P < 0,05, two-tailed unpaired *t* Test.

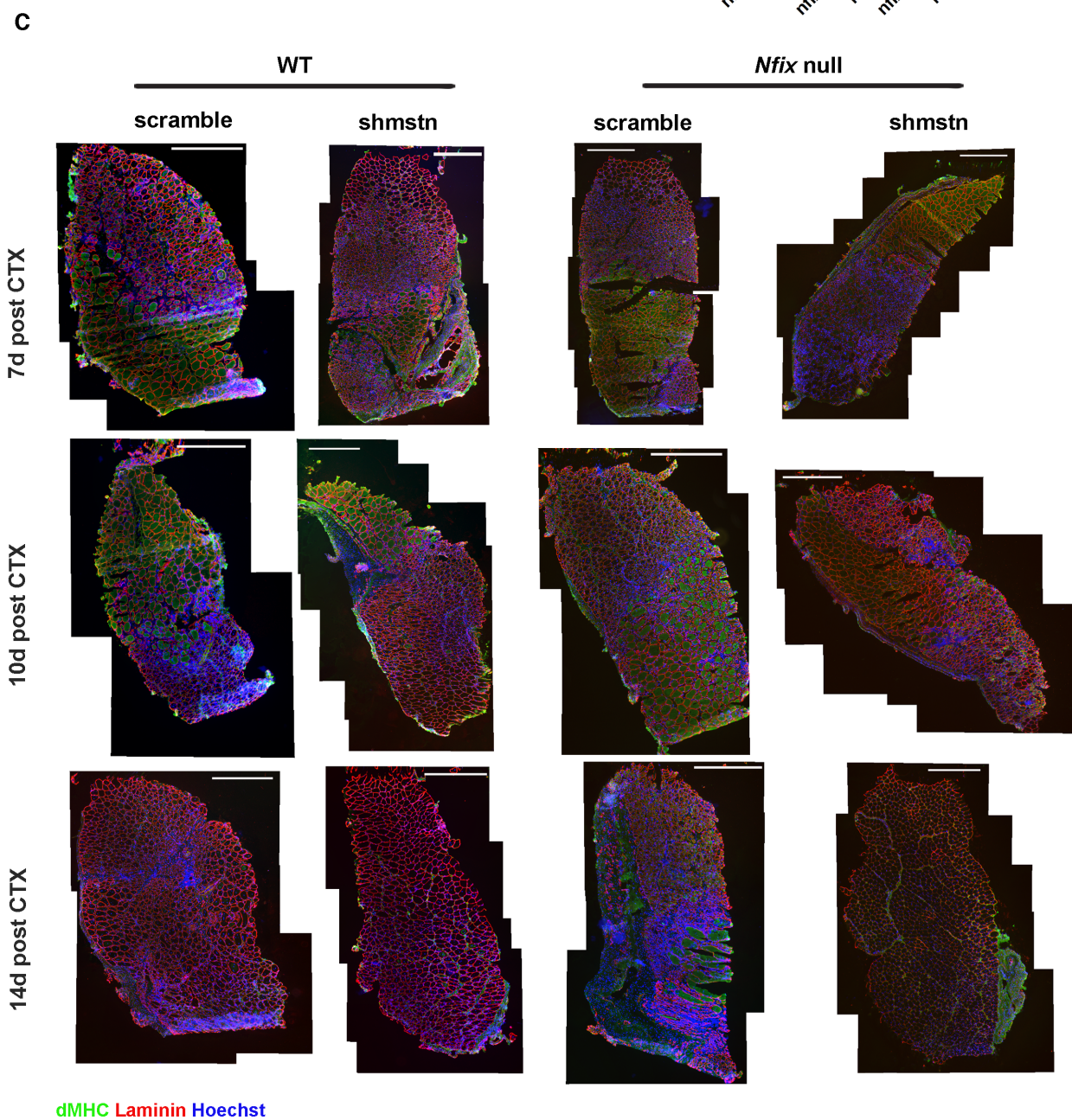
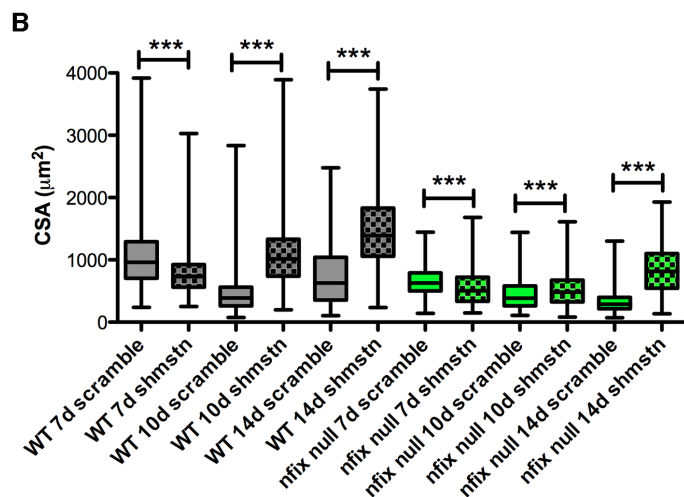
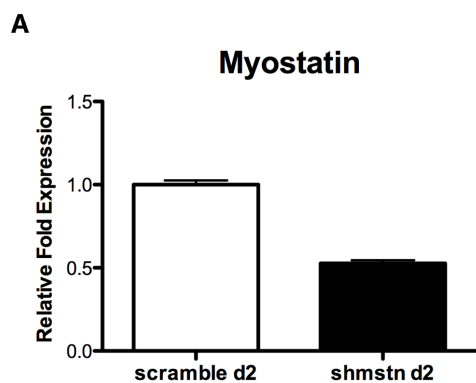


**Fig.S4. *In vivo* silencing of Myostatin rescues the regeneration defects of *Nfix* null muscles, Related to Fig.6.**

**(A)** Real-Time qPCR showing Myostatin expression in *Tibialis anterior* muscles at 2 days (d) after electroporation with control (scramble) or shMyostatin (shmstn) plasmids. Data are presented as mean  $\pm$  SD.

**(B)** Measurement of the myofiber cross sectional area distribution in WT and *Nfix* null regenerating muscles electroporated with scramble or shmstn plasmids. n=475 myofibers. Data are presented as mean $\pm$ whiskers from min to max. \*\*\*P < 0.001; two-tailed unpaired *t* Test.

**(C)** Immunofluorescence analysis of developmental MyHC expression (dMHC, green) on regenerating wild-type and *Nfix* null *Tibialis Anterior* muscle sections after muscle electroporation with a control plasmid (scramble) or with a plasmid carrying an shRNA targeting myostatin (shmstn). Muscle sections were collected and stained 7, 10 and 14 days (d) after cardiotoxin (CTX) injection. Muscles were electroporated 4 days (d) after cardiotoxin injection. Laminin, red; Hoechst, nuclei. Images represent photomerge reconstruction of the entire muscle section shown in Fig.6. Scale bar represents 500 $\mu$ m.

**Table S1. Related to Experimental Procedures. List of primers used for mouse genotyping**

| Primer Name                        | Sequence                       |
|------------------------------------|--------------------------------|
| Nfix I1F5                          | ATGGACATGTCATGGGTGCGACAG       |
| Nfix I2R2-CEC                      | AAGCCCCTCAGCTCTAGCACAGAG       |
| Nfix I1R1                          | AACCAGAGGCACGAGAGCTTGTC        |
| <i>Pax7-Cre<sup>ERT2</sup></i> for | CCACACCTCCCCCTGAACCTGAAACATAAA |
| <i>Pax7-Cre<sup>ERT2</sup></i> rev | GAATTCCCCGGGGAGTCGCATCCGCGG    |

**Table S2. Related to Experimental Procedures. List of primers used for qRT-PCR**

| Primer Name   | Sequence                |
|---------------|-------------------------|
| Myostatin for | AAGATGACGATTATGACGCTACC |
| Myostatin rev | CCGCTTGCATTAGAAAGTCAGA  |
| GAPDH for     | AGGTCGGTGTGAACGGATTG    |
| GAPDH rev     | TGTAGACCATGTAGTTGAGGTCA |

**Table S3. Related to Experimental Procedures. List of primers used for ChiP**

| Primer Name                     | Sequence                |
|---------------------------------|-------------------------|
| Myostatin promoter (415-539)for | TTGTGGAGCAGGAGCCAATC    |
| Myostatin promoter (415-539)rev | GTACCGTCCGAGAGACAACC    |
| Myostatin promoter (116-369)for | GTAACAAAACAGCACTCCAAGTC |
| Myostatin promoter (116-369)rev | CCCTGTCTGTCAACAAGTCACC  |
| Nfatc4 promoter for             | GGCGCTTAACCCTTTAGGTG    |
| Nfatc4 promoter rev             | CAAGACAGGGGAGCAGTCAC    |
| Intergenic region for           | GACCTGCCTGTTCCCTTCTTG   |
| Intergenic region rev           | GTTACCCAGCACTGCAAAGG    |